Product Focus — Cables, Connectors and Accessories

Mini-Circuits ®

ISO 9001 CERTIFIED

F 194 Rev B

PACKAGING

VARIETY

Circle 16

Applied
MICROWAVE & WIRELESS

CONTENTS

106

On Our Cover
Product Focus — Cables, Connectors and Accessories

These key RF/microwave products are constantly refined in their design and adapted to the specific needs of new applications in communications, instrumentation and system component interconnections.

Photos provided by the following companies: Andrew, Autosplice, Huber+Suhner, Microlab FXR, Schleuniger, Teledyne, Trompeter and Tru-Connector.

Editorial

The Challenge of 5 GHz Wireless Communications

By Gary A. Breed
Publisher

With the ongoing growth in wireless communications, more spectrum is needed to avoid interference and permit wider bandwidth signals. This bandwidth is required to transmit the higher data rates needed for access to the Internet or for Internet-speed personal or business information.

Where is this bandwidth? At higher microwave frequencies, of course. In the 5 to 6 GHz segment of the microwave spectrum, the FCC has allocated spectrum for both licensed and unlicensed systems capable of transmitting data at up to 20 Megabits per second, probably faster than that with new compression, encoding and modulation schemes. Development of 5 GHz wireless products is in full swing.

What are the unique features of this part of the microwave spectrum? In the middle of this range, a wavelength is a little more than 5 cm (2-1/8 in.). A paperclip is more than a half-wave long at this frequency. In free space, a conductor 1.4 mm long has an electrical length of 10 degrees. On a typical circuit board substrate or semiconductor packaging material, that is multiplied several times. Circuits need to be small, and even then, physical structures must be precisely repeatable in manufacturing.

Signal propagation is strictly line-of-sight, but multipath effects are magnified by the short wavelength and the high data rate. Antennas for these systems must have good directivity and low sidelobe radiation. Transmission losses through walls, glass and foliage increase with frequency, so most 5 GHz systems will require outdoor antennas at both ends of the path.

Fortunately, these are challenges that can be met by evolution from two current technology bases — by scaling established 2 GHz consumer hardware, and by applying innovative manufacturing methods to circuits now used in microwave point-to-point and satellite systems.

Our demands for bandwidth-to-the-home (or business) will continue to grow. As it does, 5 GHz systems will be a major step forward in the wireless industry's role in the delivery of that bandwidth. ■

The one constant
Change

And with every new format, technology, or player to enter your market, the pressure increases to keep ahead of pace. Now, perhaps more than ever, choosing the right people to collaborate with is critical. Consider someone who knows where the wireless world is heading. Agilent. We've been heavily involved with the standards boards since day one. And we're committed to giving you insight from which to base your design and manufacturing processes that's as sophisticated as your new technology. And solutions that work together across disciplines. With worldwide support and expertise wherever your teams need it. Suddenly, those market windows don't seem quite so small. **Dreams made real.**

www.agilent.com/find/wireless

u.s. 1-800-452-4844, ext. 7315
canada 1-877-894-4414, ext. 7322

Agilent Technologies
Innovating the HP Way

Circle 18

Calendar

CONFERENCES

JUNE

June 11-14, 2001
The IEEE International Conference on Communications (ICC2001)
Helsinki, Finland
Information: TSG-Congress Ltd.
E-mail: icc2001@tsgcongress.fi
Internet: http://www.icc2001.com

June 18-20, 2001
Topical Workshop and Exhibition on Flip Chip Technology
Austin, TX
Information: IMAPS
E-mail: imaps@imaps.org
Internet: http://www.imaps.org

June 20-24, 2001
Eight International Symposium on Microwave and Optical Technology (ISMOT'01)
Montreal, Quebec, Canada
Information: Professor Banmali Rawat
Tel: 775-784-6927; Fax: 775-784-6627
E-mail: rawat@ee.unr.edu
Internet: http://www.ismot2001.polymtl.ca

June 24-27, 2001
Broadband Now! — Wireless Communications Association (WCA) 14th Annual Convention
Boston, MA
Information: WCA
Tel: 202-452-7823
Internet: http://www.wca.com

June 25-27, 2001
International Engineering Consortium (IEC) ComForum: The Seamless Network
Boston, MA
Information: IEC
Tel: 312-559-4600
Internet: http://www.iec.org/events/2001/wca

JULY

July 9-12, 2001
Wireless 2001 — The 13th Annual International Conference on Wireless Communications
Calgary, Alberta, Canada
Information: Leila Southwood
Tel: 403-289-3140; Fax: 403- 282-5870
E-mail: leila@cal.trlabs.ca
Internet: http://www.trlabs.ca/wireless

July 16-17, 2001
Second IEEE European MIDAS Workshop: Topical Meeting on Mixed Signal Simulation for Communications Systems
Surrey, UK
Information: Dr. Steven Marsh
Tel: +44 1327 356426
E-mail: steve.marsh@ieee.org

July 18-22, 2001
Progress in Electromagnetics Research Symposium (PIERS 2001)
Osaka, Japan
Information: Prof. H. Ikino
Tel: +81 96 342 3851; Fax: +81 3 3259 0783
E-mail: h_ikuno@eecs.kumamoto-u.ac.jp
Internet: http://www.piers2001.gr.jp

July 24-27, 2001
2001 International Symposium on Signals, Systems, and Electronics (ISSSE 2001)
Tokyo, Japan
Information: ISSSE
E-mail: issse01@ee.kagu.sut.ac.jp
Internet: http://issse01.ee.kagu.sut.ac.jp

AUGUST

August 19-22, 2001
2001 IEEE Radio and Wireless Conference (RAWCON2001)
Boston, MA
Information: Dr. Michael S. Heutmaker
Tel: 609-639-3116; Fax: 609-639-3197
E-mail: heutmaker@lucent.com
Internet: http://rawcon.org

SEPTEMBER

September 19-21, 2001
5th International Conference on Telecommunications in Modern Satellite, Cable and Broadcasting Services (TELSIKS 2001)
Nis, Yugoslavia
Information: Dr. Bratislav Milovanovic
Tel: +381 18 529 320; Fax: +381 18 46 180
E-mail: telsiks@elfak.ni.ac.yu
Internet: http://www.telsiks.org.yu

September 24-28, 2001
European Microwave Week
London, UK
Information: Nicola Jedrej
Tel: +44 20 7861 6391; Fax: +44 20 7861 6251
E-mail: njedrej@cmp-europe
Internet: http://www.eumw.com

The part of Goliath is now being played by David.

Download a fully-functional 30-day trial (just 20MB) at www.mwoffice.com and start designing today.

The balance of power has shifted. The lumbering software of the past has finally met its match—a more agile, more accurate high frequency design solution. Microwave Office 2001. It can literally double your productivity over legacy design tools. And the precision of its models now makes first-pass success a reality. No EDA software is more powerful or intuitive either. Simple optimizations are a snap. It's easy to customize. And you get regular timely upgrades. Moreover, our schematic data translators import existing Agilent EEsof designs, so you won't lose any valuable data. For more info, visit www.mwoffice.com or call us at 310-726-3000.

AWR

Microwave Office 2001

Circle 66

Calendar

Tough Environment. Top Performance.

Stanford Microdevices has expanded its industry-leading silicon-germanium (SiGe) amplifier line with two new power devices ideally suited for driver-amplifier functions in wireless equipment operating in the most demanding signal environments.

SOT-89 Package

Offering the wireless system designer typical GaAs linearity at silicon prices, these cost-effective heterojunction bipolar transistor (HBT) units produce high output IP3 performance across the DC-3000 MHz frequency band. SGA power devices

are excellent choices for wireless infrastructure driver amplifiers, CATV amplifiers, as well as wireless-data and wireless-local-loop amplifiers. Stanford Microdevices delivers the power you need for your toughest operating environment.

For more information, visit us at stanfordmicro.com.

Part Number	Frequency Range (MHz)	Device Voltage (V)	Id (mA)	P1dB (dBm)	IP3 (dBm)	Gain @ 1 GHz (dB)	Gain @ 2 GHz (dB))	NF @ 1 GHz (dB)
SGA-9189	DC-3000	5	180	26	39	18	12	2.5
		3	165	22.5	35	18	12	2.2
SGA-9289	DC-3000	5	270	28	41	18	11	2.9
		3	315	26	39	17	11	2.6

*Data at 2 GHz unless otherwise noted

Circle 25

STANFORD MICRODEVICES

www.stanfordmicro.com • 800.764.6642

Calendar

SHORT COURSES

Besser Associates

Applied RF Techniques I
  Mountain View, CA . . . . . .June 4-8, 2001
  Mountain View, CA . . . . . .August 13-17, 2001
RF Test Equipment Operation (laboratory course)
  Mountain View, CA . . . . . .June 12, 2001
RF Testing for the Wireless Age (laboratory course)
  Mountain View, CA . . . . . .June 13-15, 2001
Receiver and Transmitter Circuit Design
  Mountain View, CA . . . . . .June 18-22, 2001
Frequency Synthesis and Phase-Locked Loop Design
  Mountain View, CA . . . . . .June 25-26, 2001
RF CMOS Design
  Mountain View, CA . . . . . .June 28-29, 2001
  Moutnain View, CA . . . . . .August 23-24, 2001
Fiber Optics Made Simple
  San Diego, CA . . . . .July 10-11, 2001
Advanced RF Power Amplifiers Techniques
  Mountain View, CA . . . . . .July 10-13, 2001
Short Range Wireless and Bluetooth
  San Diego, CA . . . . .July 10-13, 2001
  Mountain View, CA . . . . . .September 25-28, 2001
RF and Wireless Made Simple
  San Diego, CA . . . . .July 12-13, 2001
  Mountain View, CA . . . . . .August 7-8, 2001
DSP Made Simple for Engineers
  Mountain View, CA . . . . . .July 16-18, 2001
RF Transceiver Design
  Mountain View, CA . . . . . .July 24-27, 2001
Wireless Digital Communications
  Mountain View, CA . . . . . .July 30-August 3, 2001
RF and Wireless Made Simple II
  Mountain View, CA . . . . . .August 9-10, 2001
Practical Design of Integrated and Discrete Wireless Circuits
  Mountain View, CA . . . . . .August 20-22, 2001
RF Wireless System Design Fundamentals
  Mountain View, CA . . . . . .August 22-24, 2001
Bluetooth: Operation and Use
  Mountain View, CA . . . . . .August 27-28, 2001
Behavioral Modeling
  Mountain View, CA . . . . . .August 28-30, 2001
Advanced Wireless and Microwave Techniques
  Mountain View, CA . . . . . .September 10-14, 2001
Information: Annie Wong, Tel: 650-949-3300; Fax: 650-949-4400; E-mail: info@bessercourse.com; Internet: www.bessercourse.com.

TTi Technology Training Initiative (Tustin Technical Institute, Inc.)

Fundamentals of Vibration for Test
  Santa Barbara, CA . . . . . .June 4-6, 2001
Package and Product Fragility and Mechanical Shock
  Santa Barbara, CA . . . . . .June 6-8, 2001
Vibration and Shock Test Control Techniques
  Santa Barbara, CA . . . . . .June 11-13, 2001
Environmental Stress Testing for Product Reliability
  Santa Barbara, CA . . . . . .September 17-19, 2001
Digital Data Acquisition
  Santa Barbara, CA . . . . . .September 19-21, 2001
Grounding and Shielding for EMI/EMC/ESD
  Santa Barbara, CA . . . . . .September 24-26, 2001
Test Procedures for EMI/EMC/ESD
  Santa Barbara, CA . . . . . .September 26-28, 2001
Applied Measurements Engineering
  Santa Barbara, CA . . . . . .October 1-3, 2001
Metrology Concepts
  Santa Barbara, CA . . . . . .October 3-5, 2001
Calibration Processes
  Santa Barbara, CA . . . . . .October 8-10, 2001
Calibration Laboratory Management
  Santa Barbara, CA . . . . . .October 11-12, 2001
Physical Measurement Techniques
  Santa Barbara, CA . . . . . .October 15-17, 2001
Measurement Uncertainty
  Santa Barbara, CA . . . . . .October 17-19, 2001
Fundamentals of Vibration for Design
  Santa Barbara, CA . . . . . .October 22-24, 2001
Thermal Analysis and Heat Transfer
  Santa Barbara, CA . . . . . .October 24-26, 2001
Information: Brian P. Slatery, Tel: 805-682-7171; Fax: 805-687-6949; E-mail: brian@ttiedu.com; Internet: www.ttiedu.com.

Agilent Technologies

RF & Microwave Fundamentals
  Winnersh, UK . . . . .August 29-31, 2001
Network Analysis Measurements
  Winnersh, UK . . . . .October 16-17, 2001
Spectrum Analysis Measurements
  Winnersh, UK . . . . .October 18-19, 2001
Information: Tracey Bull, Tel: +44 118 9276741; Fax: +44 118 9276862; E-mail: tracey_bull@agilent.com.

Georgia Institute of Technology

RF and Wireless Principles and Practice
  Atlanta, GA . . . . .June 11-15, 2001
Adaptive Array Radar Processing
  Atlanta, GA . . . . .October 2-5, 2001
ing Education and Outreach, Tel: 404-894-2547; Fax: 404-894-7398; E-mail: conted@gatech.edu; Internet: www.conted.gatech.edu.

California State University, Northridge

Far-Field, Near-Field, Compact Ranges and Anechoic Chambers
  Northridge, CA . . . . .June 12-15, 2001
Information: Shirley Lang, Tel: 818-677-2146; Fax: 818-677-5982; E-mail: shirley.lang@csun.edu; Internet: www.ecs.csun.edu/~crs/mam/.

Calendar

University of Missouri-Rolla

Grounding and Shielding Electronic Systems
> *Boston, MA* . . . .*June 19-20, 2001*
> *Toronto, ON, Canada* . . . .*August 8-9, 2001*
> *Denver, CO* . . . .*September 17-18, 2001*

Circuit Board Layout to Reduce Noise Emission and Susceptibility
> *Boston, MA* . . . .*June 21, 2001*
> *Toronto, ON, Canada* . . . .*August 10, 2001*
> *Denver, CO* . . . .*September 19, 2001*

Information: Sue Turner, Tel: 573-341-6061; Fax: 573-341-4992; E-mail: suet@umr.edu; Internet: www.umr.edu/~conted.

University of Wisconsin at Madison

Basic Telephony and Digital Switching
> *Madison, WI* . . . .*June 19-22, 2001*

Engineering and Planning Telecommunication Local Loop Facilities
> *Madison, WI* . . . .*June 28-29, 2001*

Electrical Grounding of Communications Systems
> *Madison, WI* . . . .*August 1-3, 2001*

Information: Katie Peterson, Tel: 1-800-462-0876; Fax: 608-263-3160; E-mail: custserv@epd.engr.wisc.edu; Internet: http://epd.engr.wis.edu.

University of California at Berkeley Extension

MOSFET Physics, Technology and BSIM Models
> *Berkeley, CA* . . . .*June 20-22, 2001*

Low-Power Circuits and Systems for Digital Wireless Communications
> *Berkeley, CA* . . . .*June 28-29, 2001*

Advanced Digital Integrated Circuits
> *Berkeley, CA* . . . .*August 1-3, 2001*

Design of Analog Integrated Circuits for Mixed-Signal Integrated Systems
> *San Francisco, CA* . . . . .*August 6-10, 2001*

Information: Continuing Education in Engineering, Tel: 510-642-4111; Fax: 510-642-0374; E-mail: course@unex.berkeley.edu; Internet: www.unex.berkeley.edu/enroll.

University of California at Los Angeles Extension

Optical-Layer Networking: Key Enabling Technologies and Architectures
> *Los Angeles, CA* . . . .*July 9-11, 2001*

Satellite Communications Payload and System Design
> *Los Angeles, CA* . . . .*July 18-20, 2001*

Digital Signal Processing: Theory, Algorithms and Implementations
> *Los Angeles, CA* . . . .*August 13-17, 2001*

Information: UCLA Extension, Short Course Program Office, Tel: 310-825-3344; Fax: 310-206-2815.

International Institute of Connector and Interconnection Technology (IICIT)

Basic Connector Technology
> *Detroit, MI* . . . .*July 16-17, 2001*

Connector Failure Mechanisms
> *Detroit, MI* . . . .*July 19, 2001*

Connector Testing
> *Detroit, MI* . . . .*July 18, 2001*

Bandwidth, High Frequency and RF Effects
> *Detroit, MI* . . . .*July 19, 2001*

Information: Suzanne Romeo, Tel: 1-800-854-4248; E-mail: sromeo@iicit.org; Internet: www.iicit.org.

Process Sciences Inc.

SMT Bootcamp
> *Chicago, IL* . . . .*July 23-24, 2001*
> *Denver, CO* . . . .*August 2-3, 2001*
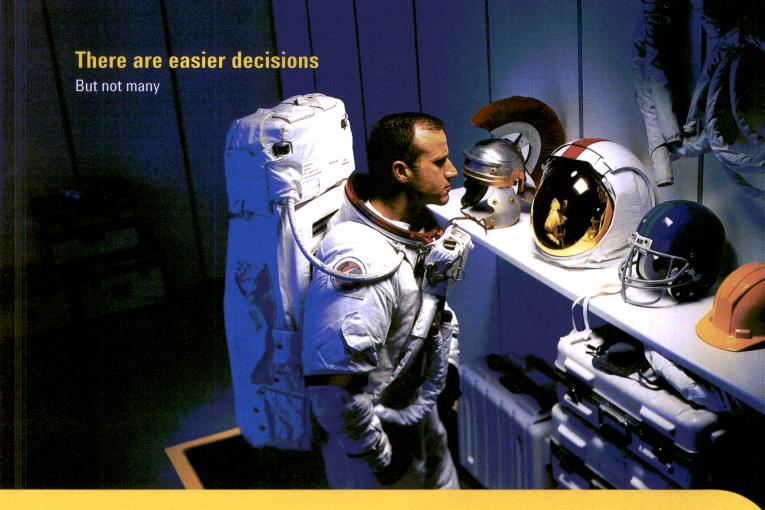
Information: Process Sciences Inc., Tel: 512-259-7071; Fax: 512-259-7073; Internet: www.process-sciences.com.

Arizona State University

Semiconductor Physics and System Reliability
> *Tempe, AZ* . . . .*September 10-13, 2001*

Information: College of Engineering and Applied Sciences, Center for Professional Development, Tel: 480-965-1740; Fax: 480-965-8653; E-mail: asu.cpd@asu.edu.

There are easier decisions
But not many

from $4,250*

Agilent 33250A

- 80 MHz bandwidth for sine and square waves
- Arb sample rate of 200 MSa/s and memory depth of 64k points
- Creates pulses up to 50 MHz quickly and accurately
- Includes modulation, GPIB, RS-232, and a 3-year warranty
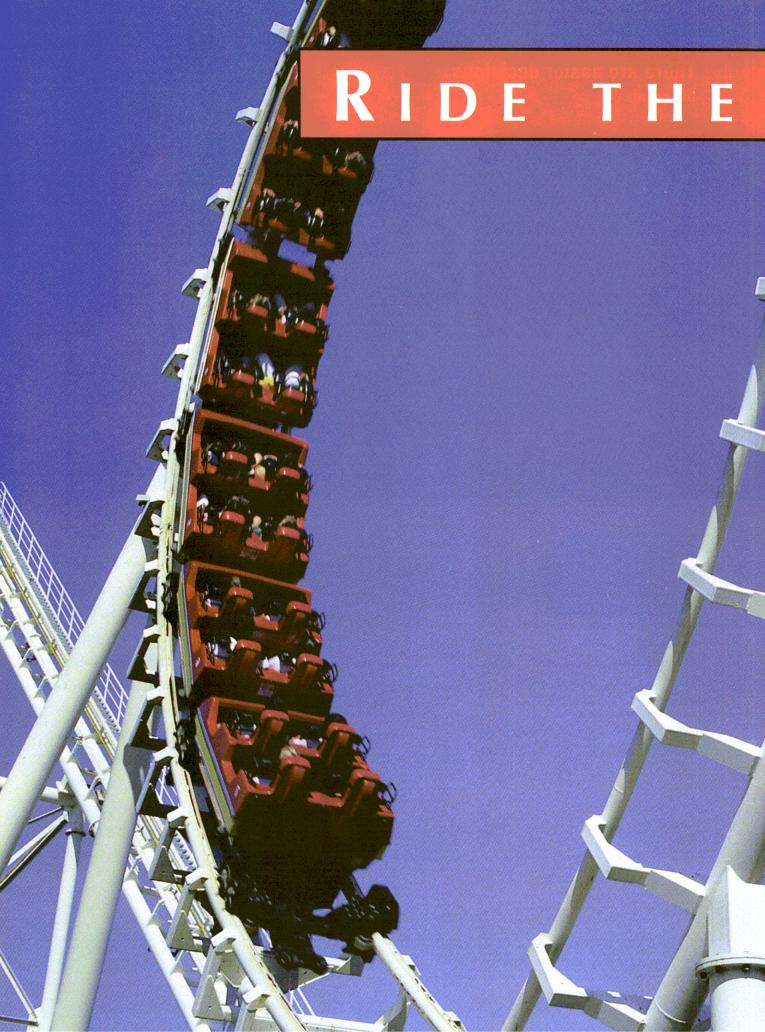
www.agilent.com/find/waveform

u.s. 1-800-452-4844, ext. 7531
canada 1-877-894-4414, ext. 7531

There are easier decisions than choosing the Agilent 33250A Function/ Arbitrary Waveform Generator, but not many. Not when, at such low cost, you can get an 80 MHz waveform generator that can produce standard waveforms, arbitrary waveforms and pulses. That has sweep, burst, modulation and external clock reference. And comes from Agilent Technologies. Now in one instrument, you have all the flexibility you need to complete your design. Along with an easy-to-use graphical color display/interface and built-in help system. Should you ever require it, you also have the help of another engineer, just by calling our toll-free number. For more information on the Agilent 33250A, you can call for a data sheet, or visit our web site for an interactive overview. With nearly double the performance and the same price as its nearest competitor, it's one decision you shouldn't have to think twice about. Dreams made real.

Agilent Technologies

RIDE THE

News

• Pentair Electronic Packaging has launched an extensive update of its Web site at www.pentair-ep.com. The redesigned site provides comprehensive technical data for design and system engineers on the company's products for enclosure and packaging applications.

• RTP Company has introduced its new P POD™ Properties Search function on the company's Web site, www.rtpcompany.com. The search is designed to quickly scan more than 2,700 compound data sheets to help customers find the right thermoplastic compound.

• Trilithic has broken ground for an expansion of its headquarters in Indianapolis, IN. The new 120,000-square-foot facility will house expanded manufacturing, research and design and administrative units, increasing the company's production capacity.

• CTS Corporation has opened a new manufacturing operation in Londonderry, NH. The 83,000-square-foot facility will supply custom backpanels and high-end systems integration services.

• Motorola Inc. and Cisco Systems Inc. have opened an Invisix™ Centre of Excellence in Bejing, China, serving customers in the Asia-Pacific region. Invisix, jointly owned by Motorola and Cisco, provides network integration services for wireless.

• Peregrine Semiconductor has opened a new design center in Melbourne, FL, specializing in high reliability and radiation effects product development.

Zentrix, University of Florida announce partnership

Zentrix Technologies and the Electrical and Computer Engineering Department of the University of Florida have announced a collaborative partnership on circuit packages. Under the program, the University of Florida will use Zentrix's low ground inductance, high performance CuPak® Circuit Packages to develop RF and microwave circuits.

The circuit packages will be used by the school's Silicon Microwave Integrated Circuits and Systems (SiMICS) Research Group, which is working to increase applications of low cost silicon-based technology in the frequency range between 1 and 30 GHz to lower the cost of communication devices.

Zentrix, based in Newburyport, MA, provides high performance RF and microwave circuit packages for wireless telecommunications.

Agilent offers short-term test equipment rental

Agilent Technologies Inc. has announced a new program designed to provide test and measurement equipment and services to customers through short-term rental. The Premier Rental Partner Program allows customers to rent Agilent's advanced test equipment for temporary needs, reducing the cost of carrying capital assets.

Agilent is in the process of selecting rental companies for the program. The first two participants are Van Nuys, CA-based Electro Rent Corporation and Dallas, TX-based CIT Technology Rentals & Services.

Agilent, based in Palo Alto, CA, provides a range of products and services for the communications and electronics industries.

Stanford Microdevices, Atmel team up for SiGe products

Stanford Microdevices and Atmel Corporation have announced a joint development agreement for the design and development of wi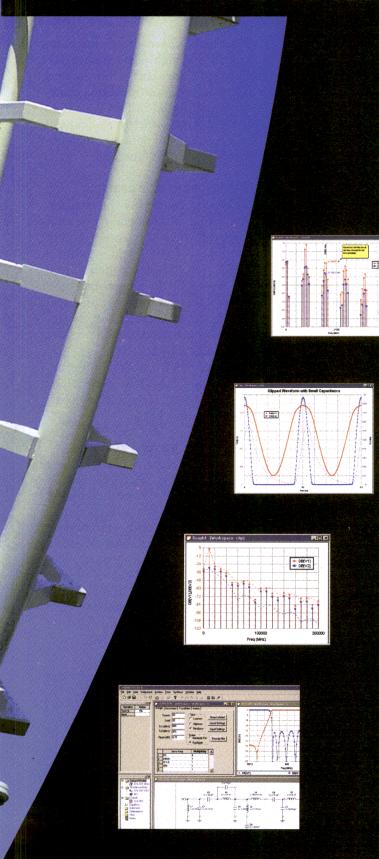reless communications products based on advanced silicon germanium (SiGe) technology. The companies plan to exchange design, packaging and test-related intellectual property to speed up the introduction of new products to their complementary consumer and wireless infrastructure markets.

Stanford, based in Sunnyvale, CA, supplies high-performance RF components for the wireless and wireline telecommunications markets. Atmel, based in San Jose, CA, designs and manufactures advanced logic, mixed-signal nonvolatile memory and RF semiconductors.

TRW announces new company

TRW has announced the creation of Velocium, a new company that will provide very high-speed indium phosphide (InP) and gallium arsenide (GaAs) components and other products for fiber optic and wireless telecommunication systems. The new company will continue TRW's InP and GaAs product development efforts.

TRW, based in Redondo Beach, CA, provides advanced technology products and services for telecommunications markets.

Anritsu offers training courses
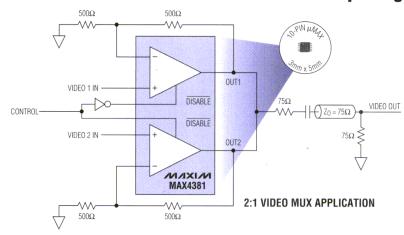
Anritsu Company is offering SiteMaster™ Training Courses on RF line sweep theory and technology. The intensive two-day course, designed for field engineers, installers and site managers, offers information on the various technologies and methodologies of line sweeping, including TDR and FDR.

Courses may be scheduled by calling 1-800-ANRITSU or by visiting the company's Web site at www.us.anritsu.com.

SMALLEST 210MHz VIDEO OP AMPS WITH DISABLE

Ideal for Low-Cost Video Multiplexing Applications

2:1 VIDEO MUX APPLICATION

IDEAL FOR...

Set-Top Boxes

Security Systems

Video Line Drivers

Video-On-Demand

Digital Cameras

SMALL
- Single Amplifier with Disable Available in Ultra-Small 6-Pin SC70

HIGH-PERFORMANCE
- 40MHz 0.1dB Large-Signal Gain Flatness is Ideal for HDTV

VERSATILE
- Operate from Single +5V or Dual ±5V Supplies

ROBUST
- Capable of Driving Up to 3 Back-Terminated 75Ω Video Lines

PART	NO. OF AMPS	DISABLE	SUPPLY VOLTAGE (V)	-3dB BANDWIDTH (MHz)	0.1dB LARGE-SIGNAL GAIN FLATNESS (MHz)	DG/DP ERROR (%/°)	PIN-PACKAGE
MAX4380/1/2	1/2/3	Yes	+4.5 to +11	210	40	0.02/0.08	6-SC70 10-µMAX/14-TSSOP
MAX4383	4	No	+4.5 to +11	210	40	0.02/0.08	14-TSSOP/SO, 16-QSOP
MAX4384	4	Yes	+4.5 to +11	210	40	0.02/0.08	20-TSSOP

FREE Video Design Guide—*Sent Within 24 Hours!*
Includes: Reply Cards for Free Samples and Data Sheets

CALL TOLL-FREE 1-800-998-8800 for a Design Guide or Free Sample
6:00 a.m. – 6:00 p.m. Pacific Time

2001 EDITION!
FREE FULL-LINE DATA CATALOG ON CD-ROM

/\/\/\XI/\/\
www.maxim-ic.com
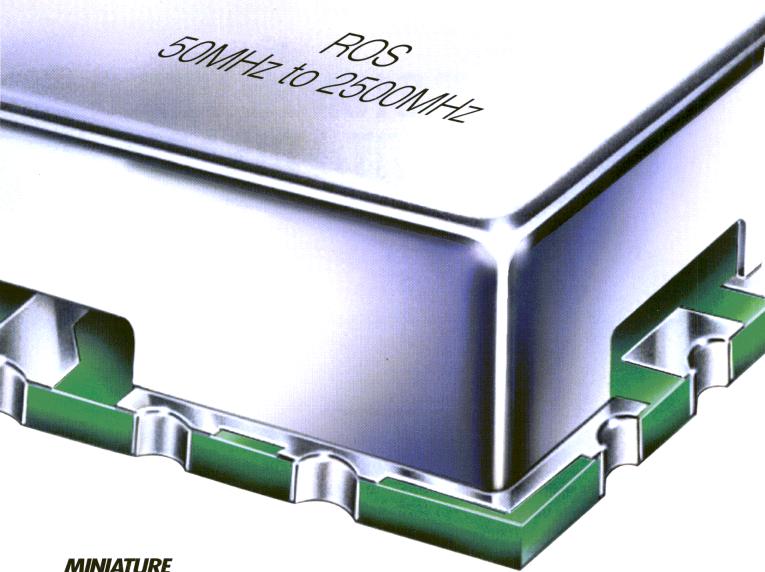
NEW! Get Price, Delivery, and Place Orders Online at www.maxim-ic.com

Circle 21 (US)   Circle 22 (International)

BUSINESS AND FINANCE

TriQuint, Sawtek announce agreement to merge

TriQuint Semiconductor Inc. and Sawtek Inc. have announced a definitive agreement for the two companies to merge. The stock transaction will have an estimate value of $1.3 billion.

TriQuint, based in Hillsboro, OR, supplies high performance gallium arsenide integrated circuits worldwide. Sawtek, based in Orlando, FL, develops and manufactures electronic singal processing components based on surface acoustic wave (SAW) technology.

Motorola wins contracts in China, Kazakhstan

Motorola Inc.'s Global Telecom Solutions Sector has announced contracts with China Mobile and China Unicom to provide network infrastructure and expansion services in several provinces, as well as a system upgrade contract in Kazakhstan.

Five of the contracts, with China Mobile Communications Corporation, call for expansion of existing GSM and GPRS networks in five provinces. The contracts, valued at $146 million, are in addition to a previously signed $213 million contract for the expansion of China Mobile's GSM 900/1800 dual band network in Hunan Province.

In a separate deal with China United Telecommunications Corp. (China Unicom), Motorola will provide 800 MHz CDMA network infrastructure in 11 provinces, including the capital, Beijing.
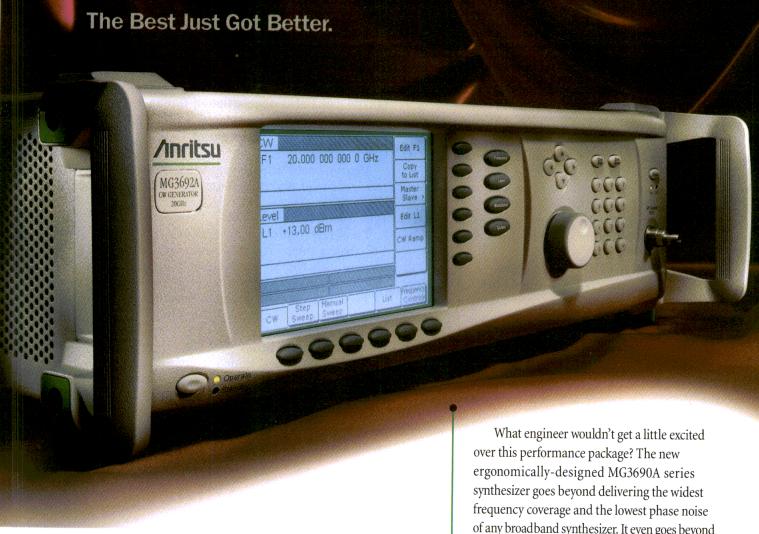
A contract with Altel in Kazahkstan covers the upgrade of the company's existing analog system to a Home Location Register (HLN) 41/Authentication system. The upgrade will provide groundwork for a future migration to CDMA technology. Terms of the agreement were not disclosed.

Motorola, based in Schaumburg, IL, provides semiconductors, integrated communications solutions, embedded electronic systems and components.

Faraday announces purchase of MetaWave Microfilters

Faraday Technology has announced that it has acquired the assets of MetaWave Microfilters. Under the agreement, the MetaWave product line will be manufactured at an expanded Faraday plant in Newcastle, Staffordshire, UK.

Faraday designs and manufactures filters, delay lines and open board signal converter products.

Circle 59

News

BUSINESS AND FINANCE

Alcatel receives contract for network in Denmark

Alcatel has been selected by Danish mobile operator Sonofon to deploy a nationwide broadband wireless network in Denmark. Under the multi-year agreement, Alcatel was also named Sonofon's exclusive LDMS provider for the company's 26 GHz spectrum license. Terms were not disclosed.

Alcatel, based in Paris, France, provides integrated voice and data networking solutions for wireless.

Siliconix to transfer DMOS switch lines

Siliconix Incorporated, a subsidiary of Vishay Intertechnology Inc., has announced plans to transfer its lines of lateral DMOS switch transistors to Linear Integrated Systems. Under the agreement, Linear Systems will support the market for the products for at least four years and will pay Siliconix royalties.

Siliconix, based in Santa Clara, CA, manufactures power MOSFETs, power ICs and analog switches for electronics and communications. Linear Integrated Systems, based in Fremont, CA, manufactures specialty linear semiconductors.

Maxim completes acquisition of Dallas Semiconductor

Maxim Integrated Products Inc. has announced the completion of its acquisition of Dallas Semiconductor Corporation.

Maxim, based in Sunnyvale, CA, develops and manufactures linear and mixed-signal integrated circuits.

Tyco acquires MultiTroniks

Tyco Electronics, a division of Tyco International Ltd., has acquired Warren, NJ-based MultiTroniks Inc., a manufacturer of automatic pick and place surface mount assembly equipment. Terms were not disclosed.

Tyco International, based in Bermuda, manufactures electrical and electronic components.

Plexus to acquire Qtron

Plexus Corp. has signed a definitive agreement to acquire Qtron Inc., a privately held electronic manufacturing services provider based in San Diego, CA. Terms were not disclosed.

Plexus, based in Neenah, WI, provides electronics design, manufacturing and testing services.

Polynomial Model of Blocker Effects on LNA/Mixer Devices

An analysis of interference effects on small-signal gain and noise figure

By William Domino, Nooshin Vakilian and Darioush Agahi
Conexant Systems

In designing today's wireless handset receivers, it is important to maximize both receive sensitivity and resistance to undesired signals, also called "interferers" or "blockers." Receiver design begins with the calculation of budgets for noise figure and linearity, usually facilitated by a spreadsheet. Although it is relatively easy to find the cascaded noise figure (NF) and 1 dB compression point (P_{1dB}) using a spreadsheet calculation, it is often not clear how to use these to predict the actual performance of the receiver in the presence of a large blocker.

A reasonably accurate prediction may instead require an inconvenient co-simulation of the system with circuit models embedded. At the level of cascade calculations rather than simulation, a simpler approach can be used.

For a digital cellular system such as Global System for Mobile Communications (GSM), well-specified blocking tests include both inband and out-of-band interferers. In these tests, the receiver front end must be able to reject the blocker while amplifying the desired signal, without exceeding the maximum allowed bit error rate. For out-of-band blockers, much of the rejection comes from a receive-band filter placed in front of the low-noise amplifier (LNA). Some designs also place a similar filter after the LNA and preceding the mixer, while others use an image-reject mixer. In the latter case, the LNA/mixer combination is often implemented as a single IC and must exhibit particularly good blocker resistance, since there is only one receive-band filter placed ahead of it.
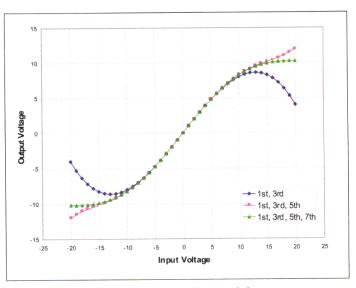
▲ **Figure 1. Polynomial compression models.**

This article discusses the effect of blockers on LNA/mixer performance. The objective is to produce a model based on empirical measurements of how an LNA/mixer's small-signal gain and noise figure degrade in the presence of large blocking signals. Once such a model is established, it can be used to accurately predict the amount of receiver desensitization resulting from varying blocker levels. The LNA/Mixer device used as an example is the Conexant RF212 dual-band image-reject downconverter for GSM.
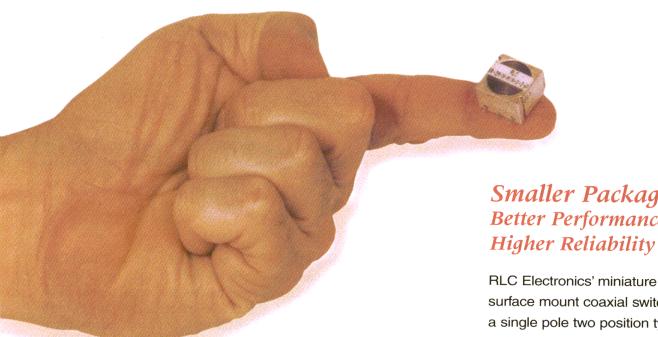
Gain compression

Typically, gain compression is only modeled as a third-order behavior, that is,

$$V_0 = k_1 V_{in} + k_3 V_{in}^3 \qquad (1)$$

SURFACE MOUNT
SPDT SWITCHES
At Your Finger Tip

Smaller Package
Better Performance
Higher Reliability

RLC Electronics' miniature surface mount coaxial switch is a single pole two position type. It combines high performance in a compact configuration. The switch provides extremely high reliability, long life and excellent electrical performance. Power consumption is less than half that of miniature connectorized switches. The SR Series is available with a choice of four different operating frequencies, two coil voltages, and two different pin configurations. RLC Electronics is ISO 9002 Certified.
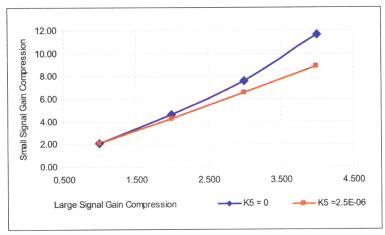
SPECIFICATIONS
SR-2min-min

SWITCH TYPE	SPDT			
Frequency (GHz)	DC-2	2-5	5-12.4	12.4-18
Insertion Loss (Max.)	0.2	0.3	0.4	0.7
VSWR (Max.)	1.3	1.4	1.5	1.7
Isolation (Min.)	70	60	50	40

Power Rating, RF Cold Switching:	10 Watts	**Life:**	1,000,000 operations
Impedance:	50 ohms	**Switching Time:**	15 milliseconds max.
Operating Power:	25° C (ma nominal)	**Environmental Conditions:**	MIL-S-3928
(Failsafe):	12 Vdc at 130 ma	**Operating Mode:**	Failsafe & Latching*
	28 Vdc at 75 ma	**Switching Sequence:**	Break before make
Connectors, RF and Power:	.018 DIA. Pins	**Weight:**	0.6 oz
		Size:	.625" x .625" x .40"H

* New Latching SPDT versions now available

TRANSFER SWITCHES ARE ALSO AVAILABLE

RLC ELECTRONICS, INC.

83 Radio Circle, Mount Kisco, New York 10549 • Telephone: 914-241-1334 • Fax: 914-241-1753
e-mail: sales@rlcelectronics.com • www.rlcelectronics.com

RLC is your complete Microwave Component source...
Switches, Filters, Power Dividers, Couplers, Terminations, Attenuators, DC Blocks, Bias Tees & Detectors

Circle 72

▲ **Figure 2. Small signal gain compression, with k_3 = .0025.**

▲ **Figure 3. Small signal gain compression, with k_3 = .0050.**

Gain compression, however, is generally a saturation-type function that cannot be completely described by the third-order component alone, which causes a downward turn of the gain curve. Figure 1 illustrates how the addition of higher order terms can produce a curve that saturates. To truly model a saturation condition would require an infinite number of terms, but a few terms, as shown in Figure 1, are sufficient to produce an adequate model. In all cases, the model cannot be used above the point where it strays from true saturation.

With first, third, fifth and seventh terms:

$$V_0 = k_1 V_{in} + k_3 V_{in}^3 + k_5 V_{in}^5 + k_7 V_{in}^7 \qquad (2)$$

To obtain the nonlinear gain, Equation (2) is divided by the input voltage.

$$Gain = k_1 + k_3 V_{in}^2 + k_5 V_{in}^4 + k_7 V_{in}^6 \qquad (3)$$

Note that the gain equation has only even-order terms. An equation of this type is particularly useful when V_{in} is a large blocker and the gain is the small-sig-

nal voltage gain in the presence of this blocker. With V_{in} always representing the blocker, the coefficients will be different for the blocker gain and the small-signal gain, since the small signal always is compressed faster than the large signal (see Appendix A).

If the transfer function model is limited to third-order and fifth-order non-linearity and the coefficients are defined as positive quantities, we can write the following equation for the large signal gain (LSG):

$$LSG = k_1 - \frac{3}{4} k_3 \left(V_{Large} \right)^2 + \frac{5}{8} k_5 \left(V_{Large} \right)^4 \qquad (4)$$

where V_{Large} is the peak amplitude of the large signal blocker. Similarly, the small-signal gain (SSG) is

$$SSG = k_1 - \frac{3}{2} k_3 \left(V_{Large} \right)^2 + \frac{15}{8} k_5 \left(V_{Large} \right)^4 \qquad (5)$$
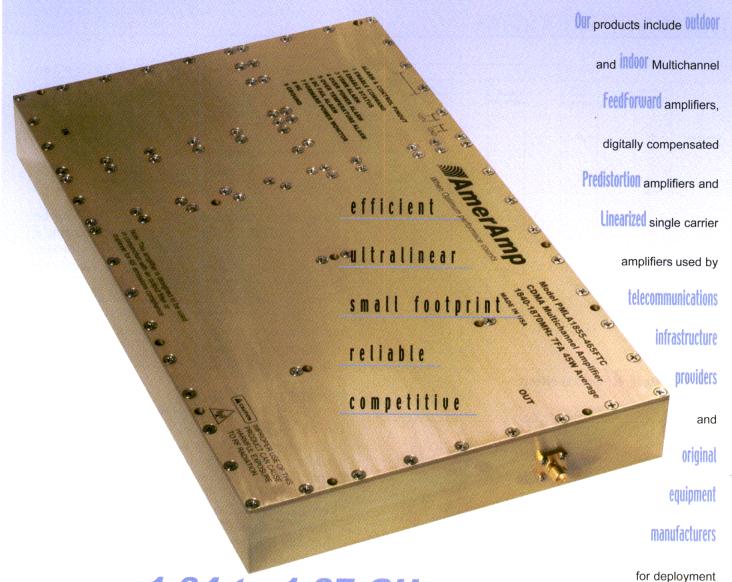
Note that the second-order term is doubled for the small signal gain, while the fourth-order term is tripled. The k_3 term causes the small signal to be compressed faster than the large signal; the k_5 term pulls the gain curve back up and keeps it from turning downward. Even though this term is tripled for the small signal gain, it is generally not enough to keep the k_3 term from causing the faster compression.

Figures 2 and 3 give some example results of compressions that occur according to Equations (2) through (5), where k_1 is unity. In these examples, two things become noticeable. First, when there is only a third-order term, the relation between SSG and LSG compression is independent of the third-order term. For instance, a compression of 1.0 dB in LSG causes a compression of about 2.1 dB in SSG, for either case of k_3, as long as $k_5 = 0$. Second, the fifth-order term has only a small influence on the relation between SSG and LSG compression until the amount of compression becomes large. This is why compression is often modeled using third-order non-linearity only.

Our approach determines the coefficients of the SSG compression by measurement and curve fit, rather than assuming they keep the precise relationship with the LSG coefficients shown in Equations (4) and (5). The noise figure increase that occurs is then measured and related to the small signal gain.

System gain and noise model

Figure 4 shows how the blocker affects the gain and noise of the system. Based on Equation (5), the blocker amplitude affects the small-signal voltage gain, as

▲ **Figure 4. Model for blocker effects.**
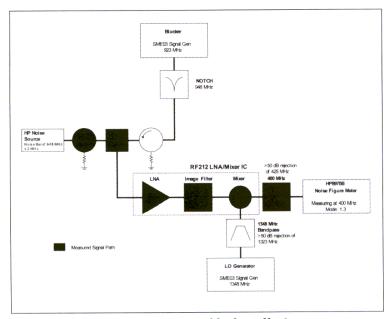
▲ **Figure 5. Test setup to measure blocker effects.**

shown by

$$SSG = a_0 - a_2(\text{Blocker})^2 + a_4(\text{Blocker})^4 \qquad (6)$$

where
  a_0 takes the place of k_1,
  a_2 takes the place of $3/2 \ (k_3)$ and
  a_4 take the place of $15/8(k_5)$.

The three noise contributors are the basic noise figure of the system, the noise figure degradation due to the blocker, and the LO phase noise mixed onto the blocker. The blocker amplitude affects the last two of these. For our modeling examples, it is most convenient to relate the noise figure degradation to the small-signal gain, which is compressed by the blocker. This relationship is best represented using zero, first and second order terms:

$$\text{Noise Factor} = n_0 - n_1(SSG) + n_2(SSG)^2 \qquad (7)$$

The blocker causes the small signal gain to be reduced while the system noise increases, causing a composite degradation in the noise figure of the system. This is taken into account when the Equations (6) and (7) are fit to actual measurements.

Finally, after the blocker is compressed, the LO noise is reciprocally mixed onto it (see Appendix B), and the noise at the blocker-desired frequency offset falls into the desired band. This noise is then combined with the other contributors.

Measurements

Figure 5 shows the test setup. Small-signal gain and NF are both measured on the HP8970B noise figure meter. The blocker generator is filtered so as not to emit noise in the desired band, and the LO generator is filtered so as not to emit noise that would mix with the blocker. Also, the IF output is filtered so the blocker does not hit the NF meter with excessive power. The combiner has isolators on either side of it. On the noise source side, the isolator protects the noise source from the blocker. On the blocker side, the isolator insures that the port sees 50 ohms both inside and outside the passband of the blocker filter.

The gain and NF with no blocker is measured, then a blocker is applied and the measurement is repeated for different blocker amplitudes. The measurements are stopped once the blocker reaches the highest value expected in the GSM system, or once the noise figure degrades by more than about 6 to 8 dB. Note that the frequencies of the measured noise band and of the blocker need to be chosen to avoid mixer spurs. If the blocker is located on or near a low-order mixer spur, then the NF meter will register an incorrect measurement.

Generating a model from the data

The gain data is converted to voltage gain and the noise figure data to noise factor, since the polynomial equations need to act upon linear quantities rather than dB. A spreadsheet is used to plot the data and produce best-fit curves. Figure 6 shows the curve for the small-signal gain versus blocker voltage for the Conexant RF212 LNA/mixer in its GSM900 path. The left-hand side of the curve is artificially constructed by folding the data over, resulting in a fit that uses all even coefficients

$$y = 3E+06x^4 + 1E-10x^3 - 7827.7x^2 - 1E-13x + 12.036$$

◆ Measured
— Poly Fit

▲ **Figure 6. Small-signal gain versus blocker voltage.**

$$y = 0.0974x^2 - 2.3704x + 16.183$$

◆ Measured
— Poly Fit

▲ **Figure 7. Noise factor versus small signal gain.**

to fit with Equation (6).

In the equation for the best-fit curve, only the even terms are significant because the curve was forced to be even. The orders of the significant terms are zero, second and fourth. The zero-order term is forced to be the same as the no-blocker gain. The equation for this curve defines the blocker dependence of the "small signal gain" box in Figure 4.
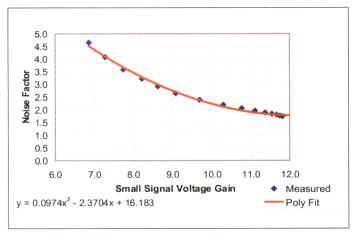
Figure 7 shows a plot of the noise factor versus small signal gain for the Conexant RF212 LNA/Mixer. The equation has terms of order zero, first and second. This equation defines (indirectly) the blocker dependence of the "noise figure degradation" box in Figure 4.

Making use of the model

Once these polynomial equations are generated, the noise contributions are summed up to determine the carrier/noise ratio (C/N) at the LNA/mixer output. An example case is shown in Figure 8, where a desired signal of −102 dBm and a blocker of −16 dBm occur on the LNA/mixer input.

To find the composite C/N, the basic quantities of gain, noise figure and P_{1dB} are required, as are the coefficients of the small-signal gain polynomial (a_0, a_2, a_4), and the noise factor polynomial (n_0, n_1, n_2). The small signal gain and the noise figure can be found based on the level of the blocker, and the reciprocally mixed LO phase noise can be added at the end.
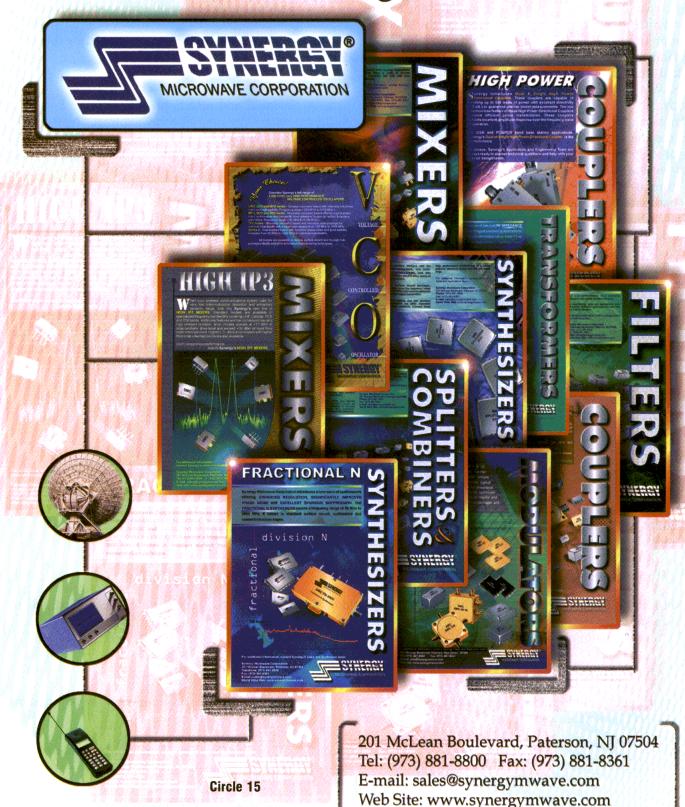
The large signal compression must be applied to the blocker itself, since in our model this compression occurs before the LO noise reciprocal mixing is applied. A polynomial with higher orders can be used for the LSG. It is useful to apply third-order distortion only for the LSG as long as the large signal does not go far beyond the P_{1dB} point of the system. Therefore, the LSG coefficients can be derived either in the same manner as the SSG coefficients, or they can be obtained from the measured P_{1dB} and the relationship in Equation (4) where $k_5 = 0$. Appendix C details the P_{1dB} derivation.

For our example, the −16 dBm blocker at the input of the Conexant RF212 LNA/Mixer causes the noise figure to degrade from 2.5 dB — the typical value with no blockers present — to 6.5 dB. The small signal gain drops from 21.6 dB to 16.75 dB. Then,

C/N = 7.8 dB

Coefficients Derived for Conexant RF212 LNA/Mixer:

Noise Factor Degradation:	Small Signal Gain:	Large Signal Gain:
n0 = 16.183	a0 = 12.040	b0 = 12.040
n1 = 2.3704	a2 = 7883.7	b2 = 3147.5
n2 = 0.0974	a4 = 3.0 x 10^6	

▲ **Figure 8. Example of model's prediction of C/N.**

the cumulative effects of the compressed SSG and NF result in a 12.5 dB C/N before the LO noise is added and reciprocally mixed onto the blocker which has been amplified by the LSG. The sum total C/N is 7.8 dB.

What makes this approach powerful is that once the model is derived, in can be plugged into the chain calculations for a complete receiver. Then, various what-if analyses can be done with accurate results for any blocker level hitting the LNA/mixer. For example, the effect of different front-end SAW filters with different levels of stopband attenuation for out-of-band blockers can be checked, and an accurate trade-off can be made between the SAW's passband insertion loss and its stopband selectivity.

Furthermore, the approach can be used to accurately estimate the sensitivity level for a receiver in the presence of a blocker. In the typical GSM receiver, the sensitivity level is where the C/N drops to about 6.0 dB. For our example with a –16 dBm blocker, the sensitivity level estimate is –103.8 dBm.

The calculation can also show which contributors are the most important. In this example, even with the seemingly high noise figure of 6.5 dB, the LO phase noise floor of –150 dBc/Hz is still the most significant contributor to the system noise, due to the blocker's presence. If the LO phase noise improves by 1 dB, then the sensitivity improves by 0.7 dB.

Conclusion

This article discussed steps in generating a polynomial model of blocker effects on small-signal gain and noise figure for LNA/mixer devices used in wireless receivers. Based on empirical measurements of gain and noise figure of the device, the polynomials relating gain compression and noise figure degradation to blocker level at the input of device were generated. The polynomial coefficients were then applied to the calculation of carrier-to-noise ratio in the presence of a blocker. The outlined approach makes it possible for a variety of what-if analyses to provide accurate results in predicting blocker-degraded C/N. ■

References

1. W. E. Sabin and E.O. Schoenike, *Single Sideband Systems and Circuits*, Second edition, New York: McGraw Hill, 1995.
2. Behzad Razavi, *RF Microelectronics*, New York: Prentice Hall, 1998.

Author information

William Domino is principal engineer for GSM RF systems engineering at Conexant Systems in Newport Beach, CA. He may be contacted via e-mail at william.domino@conexant.com.

Nooshin Vakilian is systems engineer for GSM RF Systems Engineering at Conexant Systems. She may be reached via e-mail at nooshin.vakilian@conexant.com.

Darioush Agahi is director of GSM RF Systems Engineering at Conexant Systems. He may be reached via e-mail at darioush.agahi@conexant.com.

Appendix A

Nonlinear analysis for large and small signals

Using a power series expansion, the output of a gain stage can be related to its input as

$$V_0(t) = k_1 v_i(t) + k_2 v_i^2(t) + k_3 v_i^3(t) + k_4 v_i^4(t) + k_5 v_i^5(t) + \dots\dots\dots\dots\dots \tag{a1}$$

Note that if the gain were perfectly linear, then k_1 would be the only nonzero coefficient and the gain would be identical to k_1.

For a two-tone input, $V_i(t)$ is:

$$V_i(t) = A\cos(\omega_1 t) + B\cos(\omega_2 t) \tag{a2}$$

Inserting Equation (a2) into Equation (a1) and using the well-known trigonometric equalities, the expression for $V_0(t)$ can be written as:

Low Cost, High Performance
0.5 – 3W DEVICES
For Fixed Wireless Access
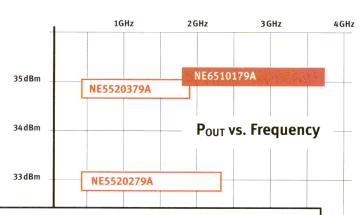
New 79A Package —
- Small size: just 4.0 x 4.2 mm
- Large grounding pad for efficient heat dissipation

New Medium Power GaAs & LDMOS FETs

- High output power, high linear gain and high efficiency.

- Low thermal resistance lets you drive your designs harder for higher linearity.

P_{OUT} vs. Frequency

NE6510179A
NE5520379A
NE5520279A

NE651R479A
NE552R479A

- Low voltage operation and miniature size make these devices ideal for wireless modems, wireless LANs, mobile radios, cordless phones, cellular phones pagers and other handheld designs.
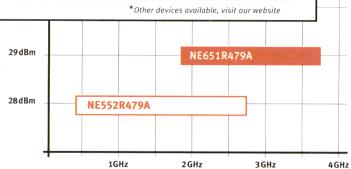
Typical Performance @ 2.3 GHz, V_{DD} = 5V

Part Number	Description	P_{1dB} (dBm)	G_L (dB)	R_{TH} (°C/W)	Freq (GHz)
NE6510179A	GaAs	35	11	5	1.8 – 3.7
NE5520279A	LDMOS	33	10	7	0.4 – 2.35
NE651R479A	GaAs	29	12	30	1.8 – 3.7
NE552R479A	LDMOS	28	11	10	0.4 – 2.7

Other devices available, visit our website

NEC | CEL

www.cel.com

$$V_0(t) = \frac{1}{2}k_2 A^2 + \frac{1}{2}k_2 B^2 + \left\{ k_1 A + \frac{3}{4}k_3 A^3 + \frac{3}{2}k_3 AB^2 + \frac{5}{8}k_5 A^5 + \frac{15}{4}k_5 A^3 B^2 + \frac{15}{8}k_5 AB^4 \right\} \cos(\omega_1 t) +$$

$$\left\{ k_1 B + \frac{3}{4}k_3 B^3 + \frac{3}{2}k_3 A^2 B + \frac{5}{8}k_5 B^5 + \frac{15}{4}k_5 A^2 B^3 + \frac{15}{8}k_5 A^4 B \right\} \cos(\omega_2 t) +$$

$$\left\{ \frac{1}{2}k_2 A^2 + \frac{1}{2}k_4 A^4 + \frac{3}{2}k_4 A^2 B^2 \right\} \cos(2\omega_1 t) + \left\{ \frac{1}{2}k_2 B^2 + \frac{1}{2}k_4 B^4 + \frac{3}{2}k_4 A^2 B^2 \right\} \cos(2\omega_2 t) +$$

$$\left\{ k_2 AB + \frac{3}{2}k_4 A^3 B + \frac{3}{2}k_4 AB^3 \right\} \cos\big((\omega_1 + \omega_2)t\big) + \left\{ k_2 AB + \frac{3}{2}k_4 A^3 B + \frac{3}{2}k_4 AB^3 \right\} \cos\big((\omega_1 - \omega_2)t\big) + \qquad \text{(a3)}$$

$$\left\{ \frac{1}{4}k_3 A^3 + \frac{5}{16}k_5 A^5 + \frac{5}{4}k_5 A^3 B^2 \right\} \cos(3\omega_1 t) + \left\{ \frac{1}{4}k_3 B^3 + \frac{5}{16}k_5 B^5 + \frac{5}{4}k_5 A^2 B^3 \right\} \cos(3\omega_2 t) +$$

$$\left\{ \frac{3}{4}k_3 A^2 B + \frac{5}{4}k_5 A^4 B + \frac{15}{8}k_5 A^2 B^3 \right\} \cos\big((2\omega_1 \pm \omega_2)t\big) +$$

$$\left\{ \frac{3}{4}k_3 AB^2 + \frac{5}{4}k_5 AB^4 + \frac{15}{8}k_5 A^3 B^2 \right\} \cos\big((\omega_1 \pm 2\omega_2)t\big) +$$

$$\frac{1}{2}k_4 A^3 B \cos\big((3\omega_1 \pm \omega_2)t\big) + \frac{1}{2}k_4 AB^3 \cos\big((\omega_1 \pm 3\omega_2)t\big) + \frac{3}{4}k_4 A^2 B^2 \cos\big((2\omega_1 + 2\omega_2)t\big) +$$

$$\frac{1}{8}k_4 A^4 \cos(4\omega_1 t) + \frac{1}{8}k_4 B^4 \cos(4\omega_2 t) \ldots\ldots\ldots$$

The two terms that are of interest are the first-order gain terms. At frequency ω_1, the output voltage is

$$V_0(\omega_1) = k_1 A + \frac{3}{4}k_3 A^3 + \frac{3}{2}k_3 AB^2 + \frac{5}{8}k_5 A^5 + \frac{15}{4}k_5 A^3 B^2 + \frac{15}{8}k_5 AB^4 \qquad \text{(a4)}$$

Similarly, at ω_2, the output voltage is

$$V_0(\omega_2) = k_1 B + \frac{3}{4}k_3 B^3 + \frac{3}{2}k_3 A^2 B + \frac{5}{8}k_5 B^5 + \frac{15}{4}k_5 A^2 B^3 + \frac{15}{8}k_5 A^4 B \qquad \text{(a5)}$$

Dividing both sides of Equations (a4) and (a5) by their respective inputs yields gain at the corresponding frequencies.

$$G(\omega_1) = k_1 + \frac{3}{4}k_3 A^2 + \frac{3}{2}k_3 B^2 + \frac{5}{8}k_5 A^4 + \frac{15}{4}k_5 A^2 B^2 + \frac{15}{8}k_5 B^4 \qquad \text{(a6)}$$
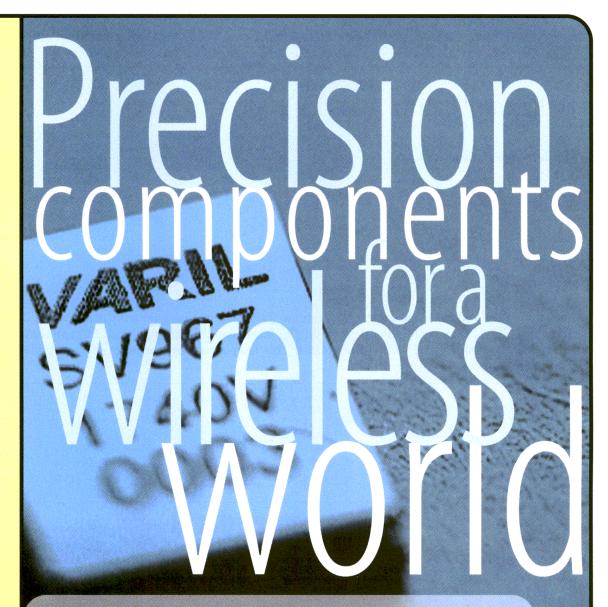
$$G(\omega_2) = k_1 + \frac{3}{4}k_3 B^2 + \frac{3}{2}k_3 A^2 + \frac{5}{8}k_5 B^4 + \frac{15}{4}k_5 A^2 B^2 + \frac{15}{8}k_5 A^4 \qquad \text{(a7)}$$

Let us assume A represents the large signal blocker and B the small desired signal. This means A>>B; therefore, we can approximate the above gain terms by letting B go to zero:

$$G(\omega_1) = k_1 + \frac{3}{4}k_3 A^2 + \frac{3}{2}k_3 B^2 + \frac{5}{8}k_5 A^4 + \frac{15}{4}k_5 A^2 B^2 + \frac{15}{8}k_5 B^4 \qquad \text{(a8)}$$

$$G(\omega_1) = k_1 + \frac{3}{4}k_3 A^2 + \frac{5}{8}k_5 A^4 \tag{a9}$$

Similarly, we can write:

$$G(\omega_2) = k_1 + \frac{3}{4}k_3 B^2 + \frac{3}{2}k_3 A^2 + \frac{5}{8}k_5 B^4 + \frac{15}{4}k_5 A^2 B^2 + \frac{15}{8}k_5 A^4 \tag{a10}$$
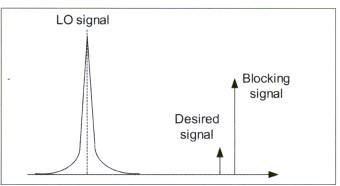
$$G(\omega_2) = k_1 + \frac{3}{2}k_3 A^2 + \frac{15}{8}k_5 A^4 \tag{a11}$$

Equations (a9) and (a11) relate the large signal gain and small signal gain respectively of an amplifier. The interesting point is that both gains depend on the large signal amplitude and, further that under large signal interference, the small signal gain suffers faster. This is apparent by comparing the coefficients of A^2 and A^4 in the above equations.

Appendix B

Reciprocal mixing

In a receiver, a small desired signal may be accompanied by a large blocking signal at some frequency offset. The local oscillator that is used to mix the desired channel to IF exhibits finite phase noise at this frequency offset. When the two signals are mixed by the LO, each one has the LO's phase noise spectrum modulated onto it. This process is referred to as "reciprocal mixing." Therefore, the downconverted band consists of two overlapping spectra, with the wanted signal suffering from significant noise overlap due to the tail of the blocking signal's spectrum.

▲ **Figure B(1). RX input signals and LO with phase noise spectrum.**
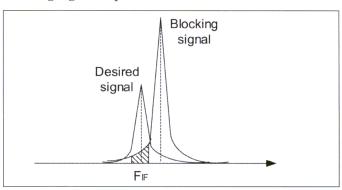
▲ **Figure B(2). Signals downconverted to IF, with overlap of reciprocally mixed noise.**

Appendix C

P_{1dB} point from third-order coefficient

To obtain the value of single-tone P_{1dB} gain compression induced by only third-order non-linearity, equation (a3) of Appendix A is used, setting higher order terms as well as signal "B" to zero.

$$V_0(\omega_1) = k_1 A + \frac{3}{4}k_3 A^3 + \frac{3}{2}k_3 AB^2 + \frac{5}{8}k_5 A^5$$
$$+ \frac{15}{4}k_5 A^3 B^2 + \frac{15}{8}k_5 AB^4 \qquad \text{(c1)}$$

Setting the higher order terms equal to zero yields

$$V_0 = \left\{ k_1 A + \frac{3}{4}k_3 A^3 + \frac{3}{2}k_3 AB^2 \right\} \qquad \text{(c2)}$$

Setting B = 0 and dividing both sides by A yields

$$V_0 = \left\{ k_1 A + \frac{3}{4}k_3 A^3 \right\} \qquad \text{(c3)}$$

$$G = \frac{V_0}{A} = k_1 + \frac{3}{4}k_3 A^2 \qquad \text{(c4)}$$

Equation (c4) is the gain with third-order nonlinearity. At P_{1dB}, the overall gain is reduced by 1 dB from the linear gain; that is, the voltage gain becomes $k_1 \times (10^{-1/20})$. To find the amplitude at P_{1dB}, we solve:

$$k_1 + \frac{3}{4}k_3 A^2 = 10^{-\frac{1}{20}} k_1 \quad \Rightarrow \quad A^2 = \frac{4}{3}\left\{ 10^{-\frac{1}{20}} - 1 \right\}\frac{k_1}{k_3} \qquad \text{(c5)}$$

Note that "A" represents the amplitude at which P_{1dB} occurs. For easier manipulation, we set
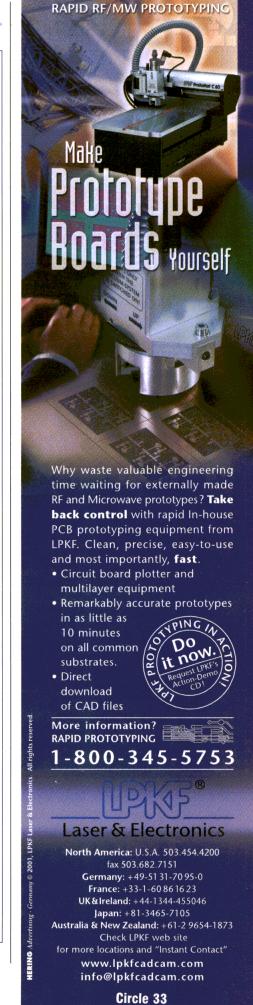
$$\alpha = \frac{4}{3}\left\{ 10^{-\frac{1}{20}} - 1 \right\} \qquad \text{(c6)}$$

Then,

$$A = \sqrt{\alpha \frac{k_1}{k_3}} \qquad \text{(c7)}$$

Equation (c7) represents the amplitude at which gain is compressed by 1 dB.

To find 1 dB compression point in terms of power, we begin with Equation (c3).

$$V_0 = \left\{ k_1 A + \frac{3}{4} k_3 A^3 \right\}$$

Next, we raise both sides to power 2.

$$V_0^2 = \left\{ k_1 A + \frac{3}{4} k_3 A^3 \right\}^2 \quad \text{(c8)}$$

After some routine arithmetic and replacing A with its equivalent α, we obtain

$$V_0^2 = \left\{ \alpha + \frac{3}{2} \alpha^2 + \frac{9}{16} \alpha^3 \right\} \frac{k_1^3}{k_3} \quad \text{(c9)}$$

Now, α can be numerically evaluated as

$$\alpha = \frac{4}{3} \left\{ 10^{-\frac{1}{20}} - 1 \right\} = -0.145$$

And V_0^2 becomes

$$V_0^2 = -0.11518 \frac{k_1^3}{k_3} \quad \text{(c10)}$$

Now V_0 is a peak voltage (we will call it V_p). Converting to dBm yields

$$P_{dBm} = 10 \log \left\{ \frac{V_p^2}{2R} 1000 \right\} = 10 \log \left\{ V_p^2 \frac{50}{R} 10 \right\} \quad \text{(c11)}$$

where R is the system source resistance.

Inserting (c10) into (c11) gives P_{1dB} in terms of the amplifier's coefficients.

$$P_{1dB} = 10 \log \left\{ -0.11518 \frac{k_1^3}{k_3} \frac{50}{R} 10 \right\} \quad \text{(c12)}$$

Since an amplifier's k_3 is a negative term, its sign can be absorbed, and the term can be presented in the absolute form, which then results in

$$P_{1dB} = 10 \log \left\{ \frac{k_1^3}{|k_3|} \frac{50}{R} \right\} + 0.614 \quad \text{(c13)}$$

In a 50-ohm system, the R becomes obsolete and P_{1dB} is reduced to

$$P_{1dB} = 10 \log \left\{ \frac{k_1^3}{|k_3|} \right\} + 0.614 \quad \text{(c14)}$$

Coupled Slot-Fed Microwave Slot Antennas on Cylindrical Substrates

By Maximilian C. Scardelletti, NASA Glenn Research Center
Thomas Weller, University of South Florida
Nihad Dib, Jordan University of Science and Technology
James Culver, Raytheon Systems
Brett King, Science Applications International Corporation

This paper describes cylindrical coupled slotline-fed (CCS-fed) slot and folded-slot antennas encompassing cylindrical substrates. Using a 1.27 cm diameter PTFE substrate, antennas that operate around 7 GHz have been realized with gains of 1.5 dB (slot) and 2.8 dB (folded slot). The antennas have a well-defined pattern null of 8 dB along the side of the CCS feedline. A 1.6 GHz slot antenna on a 1.27 cm diameter alumina substrate was also fabricated using a novel direct-write technique, which demonstrated comparable performance characteristics.

Introduction

The use of a cylindrical substrate for microwave design is generally driven by the physical attributes of the system rather than by choice, since the analysis and fabrication are more complicated than for a comparable planar implementation. However, the cylindrical geometry can offer certain desirable antenna characteristics that are not provided by planar elements. There are also a variety of configurations that can be realized, such as cylindrical conformal patch and slot antennas [1-3], microstrip [4-6] and coplanar-like transmission lines [7-10].

The CCS-fed slot antennas printed on both PTFE and alumina discussed in this article were proven to be advantageous in that an omni-directional pattern was achieved with the possibility of a well-defined null normal to the antenna axis. Thus, the antenna is well suited for use in hand-held wireless applications. In instances where the cylinder is extend-
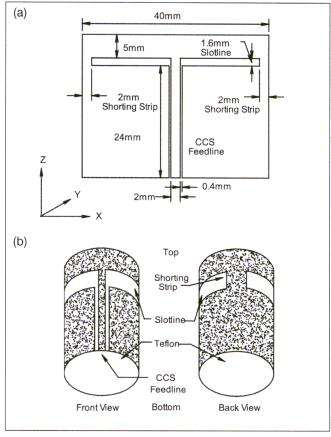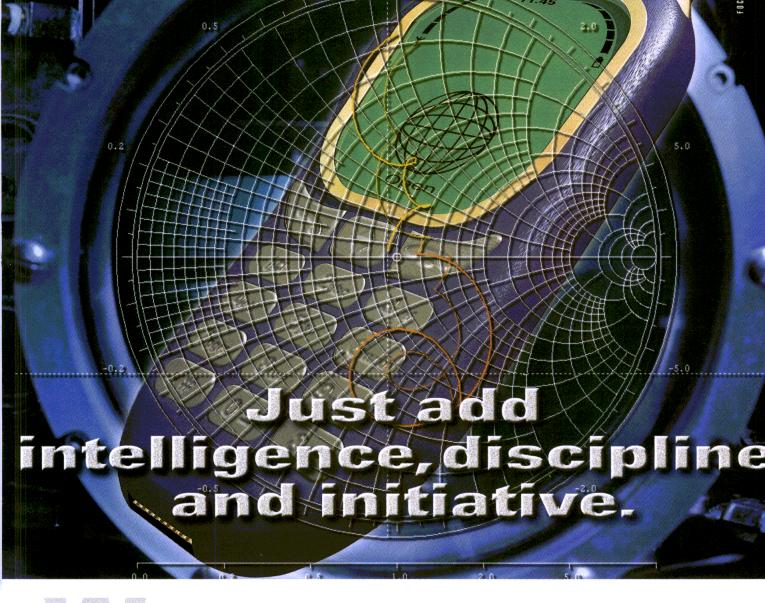
▲ **Figure 1. Cylindrical slot line antenna on PTFE: (a) two-dimensional view illustrating line and slot widths; (b) three-dimensional view with metal regions shaded (SMA connector not shown).**

ed to displace the slot antenna from other circuitry, it was also found that passive elements (filters and matching networks) can be incorporated into the otherwise unused space [8].

The first part of this article describes single-

Figure 2. Cylindrical folded slot line antenna on PTFE: (a) two-dimensional view illustrating line and slot widths; (b) three-dimensional view with metal regions shaded (SMA connector not shown).

Figure 3. Measured response of the antennas on PTFE with a 52-ohm (slot) and 40-ohm (folded slot) $\lambda_g/4$ impedance transformer.

and folded-slot antennas on PTFE designed to operate around 7 GHz. For these designs, quarter-wavelength impedance matching sections have been incorporated into the cylindrical transmission line used to feed the antennas. The gain of the single- and folded-slot antennas was 1.5 dB and 2.8 dB, respectively. The second section describes a 1.6 GHz slot antenna that was fabricated on an alumina rod using a novel direct write technology. In this case, matching was achieved by proper placement of a shorting strip along the circumference of the slot and the measured gain was 2.6 dB. Input match and pattern measurements are presented for all designs.

Slot antennas on PTFE
Geometry and fabrication
The cylindrical slot- and folded-slot antenna designs for the PTFE substrate are shown in Figures 1(a) and 2(a). The antennas were constructed with a conductive strip across the radiating slotline and placed opposite the CCS center conductor. The CCS feedline dimensions are 2 mm for S and 0.4 mm for W. The CCS dimensions correspond to a characteristic impedance of 76 ohms, as

determined from a conformal mapping program [11]. Three-dimensional views of the antennas are illustrated in Figures 1(b) and 2(b).

The antennas were fabricated on a thin microwave substrate material with a dielectric constant (ε_r) of 2.06 [12]. The chosen substrate has a copper conductor thickness of one-third ounce (12 μm) and a dielectric thickness of 3 mils (76.2 μm). After processing, the thin substrate was wrapped around the cylindrical PTFE rod and soldered to form a continuous ground plane on the side opposite the feedline. An SMA connector was fastened to one end of the dielectric rod and soldered to the CCS center conductor and ground planes.

Antenna performance
The return loss of each antenna was measured on a Hewlett-Packard 8510 Vector Network Analyzer (VNA) following a Thru-Reflect-Line (TRL) calibration using CCS standards. Input impedances around the 7 GHz resonance frequency were determined to be 36 ohms for the slot and 21 ohms for the folded slot. In order to improve the match to the 76 ohms reference impedance, $\lambda/4$ impedance transformers were incorporated into the feedlines of the antennas. The return loss for the modified antennas is shown in Figure 3. The center frequency occurs at the point when the slot circumference is approximately λ_g, where λ_g is the guide wavelength using an effective dielectric constant of 1.5 for the slotted region [10].

The H-plane patterns for the slot are shown in Figure 4; the folded slot antenna is shown in Figures 5. (The H-plane corresponds to the x-y plane, as indicated in Figures 2(a) and 3(a).) In each case, a well-defined null occurs around the $\phi = 0$ degree direction, corresponding to the feedline side of the cylinder. The pattern asym-

▲ **Figure 4. H-plane slot antenna radiation pattern with CCS feedline side of antenna referenced to 0 degrees.**
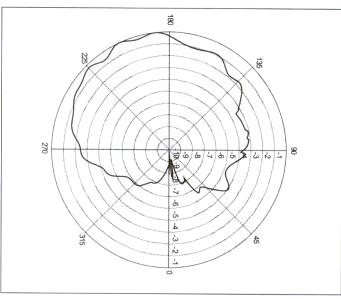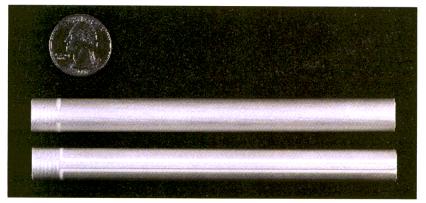
▲ **Figure 5. H-plane folded slot antenna radiation pattern with CCS feedline side of antenna referenced to 0 degrees.**

▲ **Figure 6. Photograph of the cylindrical slot antennas fabricated on 1.27 cm diameter alumina rods. The upper image shows the shorted ends of the slot on the back side of the antenna. The lower image shows the cylindrical coupled slot feedline.**

metry could be related to the feedline discontinuities, and the deep cancellation may be due to destructive interference through the center of the cylinder; at 7 GHz, the rod diameter corresponds to $\sim \lambda_g/2$ using the $\varepsilon_r = 2.06$ dielectric constant.

Due to the relatively short length of the CCS feedline and the presence of the SMA connector, it was not possible to accurately measure E-plane patterns. Using a standard gain horn as the reference antenna, the maximum gain was determined to be 1.48 dB for the slot and 2.84 dB for the folded slot.

Slot antenna on alumina
Geometry and fabrication
As illustrated in Figure 6, the slot antenna (1.5 mm

width) extends partially around the circumference of the 1.27 cm diameter cylinder where it is terminated by a shorting strip with a 4.8 mm arc length. The coupled slot-line (CCS) feed has 1.14 mm wide slots separated by 2.5 mm. The characteristic impedance of the feedline is 50 ohms.

The alumina substrate for a cylindrical slot antenna offers the advantages gained by a high ε_r material without the problems often encountered with microstrip patch or planar slot antennas. In this example, the $\varepsilon_r = 9.8$ material provides a relatively small (1.27 cm diameter) antenna with a resonant frequency at 1.6 GHz. Unlike a microstrip patch, the radiation efficiency is not adversely affected by surface mode propagation in the high ε_r material. Unlike a planar slot, the problems associated with reflections at dielectric boundaries (often leading to the use of a dielectric lens) are not encountered, since the cylindrical slot radiates into free-space, rather than into the substrate. One precaution with the cylindrical geometries is to operate below the cutoff frequency of the dominant waveguide mode, which in this case is at 4.4 GHz [9].

The antenna was fabricated using a prototype direct write tool capable of depositing metals and dielectrics directly onto conformal surfaces. This tool is known as the MesoTool and includes deposition techniques for both thick and thin film applications. It comprises two separate instruments: the MicroPen for thick film paste dispensing and the Laser Chemical Vapor Deposition (LCVD) for thin film deposition. (The development of

SV MICROWAVE™
RF Connectors & Components

HAS YOUR RF CONNECTOR SUPPLIER...

a) Been swallowed up by a huge conglomerate?

b) Moved to a new location and lost the recipe?

c) Changed names and forgotten yours?

If so, SV Microwave can solve your problems by providing:

- An accessible engineering staff
- A supportive and helpful sales team
- Quick responses
- Short lead times
- Direct equivalents
- An array of Mil Qualified items

Tired of being treated like a number? Feeling misplaced in the confusion? Being turned away on special design projects? Give us a call. We haven't lost the personal touch!

Visit our website:
www.svmicrowave.com

3301 Electronics Way, West Palm Beach, Florida 33407
Tel: 561-840-1800 • Fax: 561-842-6277 • E-mail: sales@svmicro.com

Circle 17
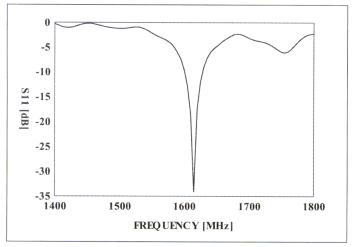
▲ **Figure 7. Measured input reflection coefficient (S₁₁) for the cylindrical slot antenna on alumina.**

▲ **Figure 8. Measured H-plane gain pattern for the cylindrical slot antenna on alumina. The feedline location is indicated by the dashed line centered around 90 degrees, while the shorted slot section is indicated by the solid line centered around 348 degrees.**

▲ **Figure 9. Measured E-plane gain pattern for the cylindrical slot antenna on alumina. The top of the cylindrical alumina rod corresponds to 0 degrees.**

this tool is currently being funded by U.S. DARPA.)

The MicroPen is a tool capable of dispensing pastes with a vast range of viscosities (0.001 to 900 Pascal/seconds). The line width resolution of the pen varies from 50 μm to several millimeters. The MesoTool dispenses and then sinters the paste that is deposited with laser heat. Currently, silver pastes are available that can be processed with a laser at 200 degrees Celsius. We used the MicroPen to deposit 37 micron-thick silver lines on the alumina substrate. LCVD can be used to deposit thin films with higher resolution than the MesoTool; line widths in the submicron range are possible. This deposition method can lay down patterns in both two and three dimensions. In addition to growing lines on a flat or curved surface, LCVD also allows growth of vertical lines, thus enabling new possibilities in the area of antenna design. In addition, LCVD permits the deposition of several metals (for example, gold, copper and tin) and dielectric materials.

Antenna performance
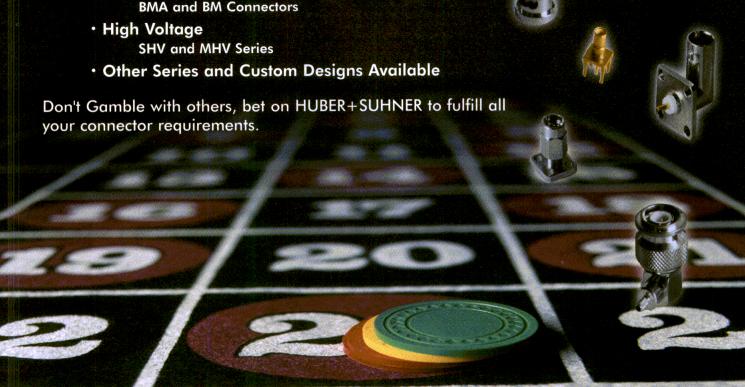
By varying the position of the shorting strip relative to the feedline, it is possible to change the input impedance of the antenna. In this design, the optimum location for the center of the shorting strip was found to be approximately 110 degrees from the center of the feedline. At the resonant frequency of 1.6 GHz, the resulting configuration is a slot length of 0.44 guide wavelengths around the cylinder with a feedpoint at 0.125 guide wavelengths from one end. With respect to this offset feed arrangement, one advantage of the cylindrical ground plane is that the parasitic even-mode on the CCS feedline is naturally suppressed. For a comparable uniplanar coplanar waveguide, air-bridges would be required at the feedpoint to equalize the ground planes. The measured input reflection coefficient (S₁₁) is given in Figure 7. The 10 dB return loss bandwidth is approximately 2 percent.

The measured H-plane gain patterns of the antenna are shown in Figure 8, while E-plane gain patterns of the antenna are given in Figure 9. The H-plane pattern, measured around the cylinder, shows a variation between 0 and 2.6 dBi, with the minimum gain occurring approximately opposite the shorting strip. While the location of the pattern minimum is consistent with

the results for the antennas on PTFE (opposite the short) the null is not nearly as well defined in this case. This may be explained by differences in the interaction of radiated fields from opposing sides of the cylinder; unlike the PTFE case, the rod diameter is not near a multiple of $\lambda_g/2$ at the resonant frequency (using a dielectric constant of 9.8) and thus less cancellation occurs. The E-plane pattern resembles that of a linear dipole, with the null occurring along the central axis of the cylinder. Some distortion in the E-plane pattern can be attributed to the coaxial connector used to connect to the alumina rod.

Summary

Cylindrical slot and folded slot antennas on PTFE and alumina have been presented. The antennas exhibit broad beamwidths with the possibility for well-defined pattern nulls normal to the axis of the CCS. This type of antenna is useful as a linear dipole replacement when low profile and broadside radiation are desired. A powerful direct-write manufacturing tool capable of depositing metals and dielectrics on virtually any conformal surface has been described. ■

References

1. J. Jain-Ming, J. A. Berrie, R. Kipp, and S. Lee. "Calculation or Radiation Patterns of Microstrip Antennas on Cylindrical Bodies of Arbitrary Cross Section," *IEEE Transactions on Antennas and Propagation*, Vol. 45, No. 1, January 1997: 126-132.

2. J. M. Jarem and N.J. Sheikh. "Pattern Synthesis of Cylindrical Slot Antenna," *Electronics Letters*, Vol. 16, No. 10, May 1980: 383-385.

3. C.H. Ho, P.K. Shumaker, L. Fan, K.B. Smith and J. W. Liao. "Printed Cylindrical Slot Antenna for Commercial Applications," *Electronics Letters*, Vol. 32., No. 3, February 1996: 151-153.

4. N. G. Alexopoulos and A. Nakatani. "Cylindrical Substrate Microstrip Line Characterization," *IEEE Transactions on Microwave Theory and Techniques*, Vol. MTT-35, No. 9, September 1987: 843-849.

5. H. A. Auda and A. Z. Elsherbeni. "Multiple Microstrip Lines on a Multilayered Cylindrical Dielectric Substrate on Perfectly Conducting Wedge," *IEEE Transactions on Microwave Theory and Tech-niques*, Vol. MTT-41, No. 9, September 1993: 1037-1043.

6. J. Huang, R. Vahldieck and H. Jin. "Microstrip Discontinuities on Cylindrical Surfaces," *IEEE MTT-S Symposium*, Vol. 3, June 1993: 1299-1302.

7. H. Su and K. Wong. "Dispersion Characteristics of Cylindrical Coplanar Waveguides," *IEEE Transactions on Microwave Theory and Techniques*, Vol. MTT-44, No. 11, November 1996: 2120-2122.

8. N. Dib and T. Weller. "Finite Difference Time Domain (FDTD) Analysis of Cylindrical Coplanar Waveguide (CCPW) Circuits," *International Journal of Electronics*, Vol. 87, No. 9, September 2000: 1083-1094.

9. N. Dib, T. Weller and M. Scardelletti. "Analysis of 3-D Cylindrical Structures Using the Finite Difference Time Domain Method," *IEEE MTT-S Symposium Digest*, June 1998 (Baltimore, MD): 925-928.

10. N. Dib, T. Weller, M. Scardelletti and M. Imparato. "Analysis of Cylindrical Transmission Lines with the Finite Difference Time Domain Method," *IEEE Transactions on Microwave Theory and Techniques*, April 1999: 509-512.

11. N. Dib and A. Al-Zoubi. "Quasi-Static Analysis of Asymmetrical Cylindrical Coplanar Waveguide with Finite-Extent

Ground," *International Journal of Electronics*, Vol. 87, No. 2, February 2000: 185-198.

12. *CuFLON Microwave Substrate Primer: Technical Bulletin #1*, Polflon Company CT, 1997.

Author Information

Maximilian C. Scardelletti received bachelor of science and master of science degrees in electrical engineering from the University of South Florida in 1997 and 1999, respectively. He is currently enrolled at Case Western Reserve University in Cleveland, OH, where he is working towards his doctoral degree in RF and microwave microelectromechanical systems (MEMS). In August 1999, he joined the staff of the Communication Technology Branch at NASA Glenn Research Center in Cleveland. His interests include the development and characterization of RF and microwave MEMS, coplanar printed antennas and RF andMicrowave passive components.
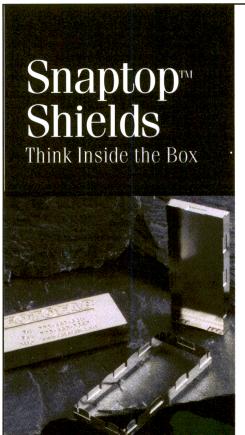
Thomas Weller is an assistant professor of electrical engineering at the University of South Florida. He received his Ph.D. in electrical engineering from the University of Michigan in 1995. His current research interests include microwave MEMS and micromachining, planar circuit and antenna design and microwave modeling. He has published more than 75 technical papers. He can be reached at E-mail: weller@eng.usf.edu, Tel: 813-974-2440 and Fax: 813-974-5250.

Nihad Dib is an associate professor of electrical engineering at Jordan University of Science and Technology. He received his Ph.D. in electrical engineering from the University of Michigan in 1992. His research interests include computational electromagnetics, antenna design and modeling of passive microwave circuits.

James Culver has 16 years of experience in micro-wave circuit and systems design, including five years with Texas Instruments developing narrow and wide band monolithic microwave integrated circuits (MMICs) for use in radar and communication systems. In addition to design, he has extensive experience with linear and nonlinear modeling of active devices and in numerical electromagnetic modeling of passive structures. He is employed as a principal engineer with Raytheon Systems Company, where he designs microwave communications systems. He has a bachelor of arts degree in chemistry, a bachelor of science degree in electrical engineering and a master of science degree in electrical engineering. He is currently pursuing a doctor of philosophy degree in electrical engineering in the area of microelectromechanical systems (MEMS) applied to microwave circuits and antennas. He holds one patent and has authored 15 papers on MMIC and microwave circuit design.

Brett King is an RF and microwave engineer with five years of experience in high-frequency design with Raytheon Systems Company. He is currently employed with Science Applications International Corporation (SAIC). His experience includes work on amplifier design, passive element and transmission line modeling, high reliability space applications and communication systems integration. He has a bachelor's degree in electrical engineering from the University of South Florida and is currently pursuing a master's degree (MSEE).

Measuring Complex Permittivity of Materials for Frequencies Under 18 GHz
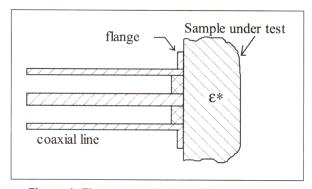
By Israel Garcia-Ruiz and Carlos David Aviles-Castro, Centro Nacional de Metrologia; and Hildeberto Jardon-Aguilar, CINVESTAV del IPN

This article describes two systems for the measurement of complex permittivity of solids and other materials for the 100 MHz to 18 GHz frequency range. One system is based on a coaxial probe and the other on the measurement of reflected and transmitted waves with antennas. The dielectric characteristics of Teflon® PTFE and Rexolite 4422 were measured and compared with both systems, and a good agreement was found. As will be shown, the open-ended coaxial technique is also appropriate for testing low-loss solids; the free-space technique, mainly used for millimeter and quasi-optical systems, can also be applied for the lower part of the microwave range. Implantation details, as well as material characterization results, are provided.

Introduction

Complex permittivity is a crucial parameter in many RF and microwave applications [1] for making reasonably accurate wide-band and quick measurements. Several techniques have been developed for measuring complex permittivity [1-3]; however, some, such as resonant cavity or wave-guide transmission line cells, require test hardware machining and meticulous sample preparation. In addition, these techniques are destructive and have a limited frequency range.

Open-ended coaxial probe and free-space techniques have been used to characterize dielectric properties of materials [4-7]. The coaxial probe has proved to be more suitable for materials such as liquids, soft solids, powders and tissues, because good contact at the interface is easier to achieve. On the other hand, the free-space measurement system using horn
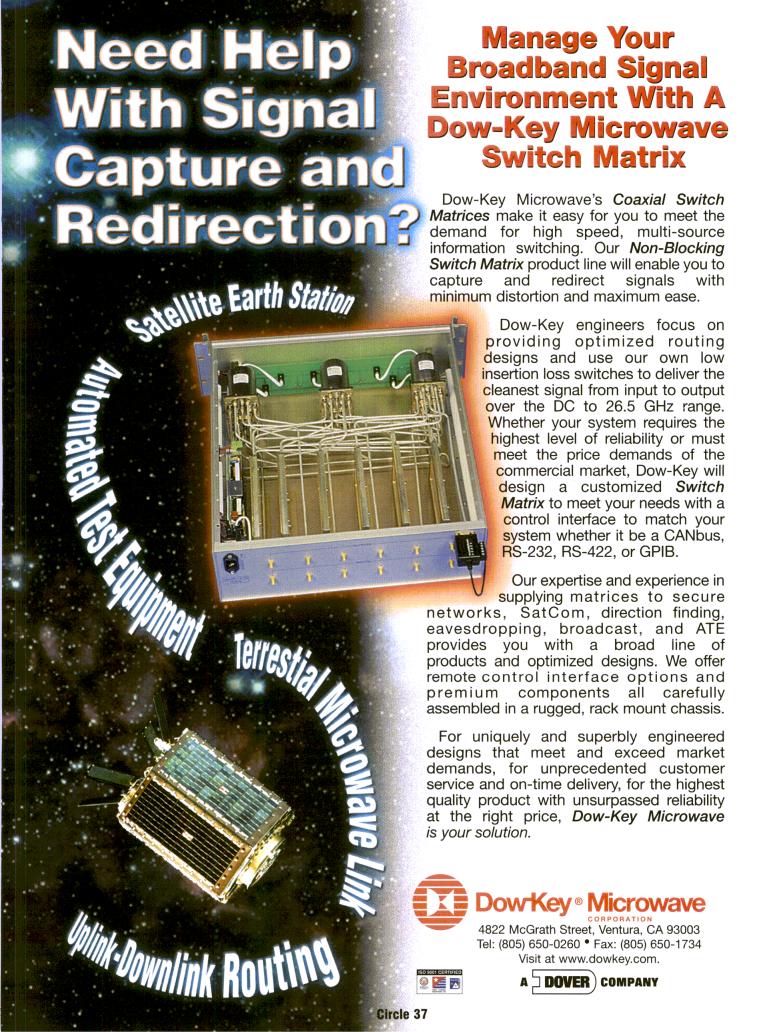
▲ **Figure 1. The open-ended coaxial probe.**

antennas is a non-contact implementation that has found applications for characterization of materials such as low loss plastics, microwave absorbers and substrates.
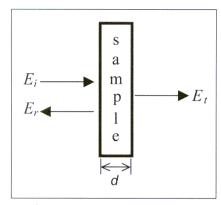
Traditionally, several approaches have been used to calculate permittivity from reflection coefficient measurements using the coaxial probe: full-wave analysis [4-7], lumped circuit modeling [8] and antenna modeling [8] of the probe. The open-ended coaxial probe technique, however, is not definitive because it depends on the use of reference materials to calibrate the measurement system or ensure the solution convergence. The free-space method is more exact because it depends only on the use of the electromagnetic theory equations and on how closely the experimental system realization reproduces the conditions stated by the equations and the accuracy of reflection and transmission coefficients measurement.

The open-ended coaxial probe technique

The main advantage of coaxial probes is their wide-band frequency response. When applying

Need Help With Signal Capture and Redirection?

Satellite Earth Station

Automated Test Equipment

Terrestial Microwave Link

Uplink-Downlink Routing

Manage Your Broadband Signal Environment With A Dow-Key Microwave Switch Matrix

Dow-Key Microwave's *Coaxial Switch Matrices* make it easy for you to meet the demand for high speed, multi-source information switching. Our *Non-Blocking Switch Matrix* product line will enable you to capture and redirect signals with minimum distortion and maximum ease.

Dow-Key engineers focus on providing optimized routing designs and use our own low insertion loss switches to deliver the cleanest signal from input to output over the DC to 26.5 GHz range. Whether your system requires the highest level of reliability or must meet the price demands of the commercial market, Dow-Key will design a customized *Switch Matrix* to meet your needs with a control interface to match your system whether it be a CANbus, RS-232, RS-422, or GPIB.

Our expertise and experience in supplying matrices to secure networks, SatCom, direction finding, eavesdropping, broadcast, and ATE provides you with a broad line of products and optimized designs. We offer remote control interface options and premium components all carefully assembled in a rugged, rack mount chassis.

For uniquely and superbly engineered designs that meet and exceed market demands, for unprecedented customer service and on-time delivery, for the highest quality product with unsurpassed reliability at the right price, *Dow-Key Microwave is your solution.*

Dow-Key® Microwave
CORPORATION

4822 McGrath Street, Ventura, CA 93003
Tel: (805) 650-0260 • Fax: (805) 650-1734
Visit at www.dowkey.com.

ISO 9001 CERTIFIED

A DOVER COMPANY

Circle 37

▲ Figure 2. Diagram showing incident, reflected and transmitted waves.

the open-ended coaxial probe approach, good contact at the interface of the probe with the material under test is necessary. Therefore, coaxial probes may have been used more extensively for liquids, such as alcohol, water, saline solutions and oil, and soft solid materials, including organic tissues such as human skin, as well as vegetables and powders, where such a good contact can be assured. In the case of solid materials, an air gap at the interface often introduces measurement errors. Several works have been devoted to evaluate the extent of these errors, and results can be found in literature. It was shown in [9] that an average surface roughness of 1 μm produces an error of about 1 percent in the dielectric constant value of Teflon, with respect to the value that would correspond to zero roughness. Then, good contact and a smooth surface have to be assured.

A schematic for a coaxial open-ended probe is shown in Figure 1. The material being tested is placed in close contact with the probe's flat end; the reflection coefficient, measured with a vector network analyzer (VNA) or some other reflectometry technique, is related to the complex permittivity of the material, as shown in Equation (1).

$$\Gamma^*\left(\omega,\varepsilon^*\right)=\frac{Z_S-Z_0}{Z_S+Z_0} \tag{1}$$

where ω is the angular frequency, Z_S is the probe impedance and Z_0 is the characteristic impedance.

To calculate ε^* from the impedance measurements or the reflection coefficient, the bilinear calibration model, proposed first by Cole [10], is used. This model, an extension of the bilinear transformation used in microwave circuit theory [11], can also be seen as an equivalent circuit model incorporating a two port error correction box. Using this model, ε^* can be expressed by Equation (2):

$$\varepsilon^*=\frac{A\rho+\varepsilon^*_{ref}}{1-B\rho} \tag{2}$$

where

$$\rho=\frac{\Gamma_{ref}-\Gamma_x}{\Gamma_{ref}+\Gamma_x}$$

and A and B are calibration constants that are calculated using two reference materials, ε^*_{ref} and Γ_{ref} are the permittivity and reflection coefficient of a known reference material; and Γ_x and ε^* are the reflection coefficient and permittivity of the material being tested.

The bilinear calibration model is very convenient, equations are linear and simple to solve and reasonably accurate results can be obtained if several considerations are taken into account. Suitable reference materials to solve Equation (2) have to be chosen, their permittivity values have to be well known and evenly distributed around expected values, calibration has to be carefully performed and good contact has to be assured at the probe interface.

The free-space technique

When a plane wave is striking a slab of material of thickness d, as shown in Figure 2, the wave will be partially reflected back and partially transmitted across the material. Similar to wave-guided systems, reflected and transmitted fractions can be characterized by means of a reflection and a transmission coefficient.

The reflection coefficient can be written as (see Figure 2):

$$\Gamma=\frac{E_r}{E_i}$$

while the transmission coefficient can be written as:

$$\tau=\frac{E_t}{E_i}$$

where E_i, E_r and E_t represent the amplitudes of electric fields of incident, reflected and transmitted waves, respectively. The ratios expressed depend on the dielectric properties of the material. Their relationship can be expressed by using Equations (3) and (4) [11, 13]:

$$\Gamma=\frac{1-\sqrt{\varepsilon^*}}{1+\sqrt{\varepsilon^*}} \tag{3}$$

$$\tau=e^{-\gamma d} \tag{4}$$

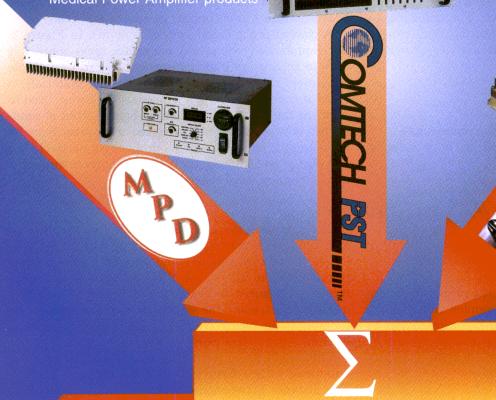where γ is the complex propagation constant. It is defined as

$$\gamma=\alpha+j\beta=j\frac{2\pi}{\lambda_0}\sqrt{\varepsilon^*} \tag{5}$$
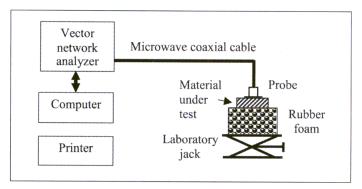
▲ Figure 3. Permittivity measurement system based on a coaxial probe.

Dielectric information can be extracted either from Equation (3), Equation (4), or both. The transmission coefficient is also a complex quantity that can be expressed in polar format equations, as shown in Equation (6):

$$\tau = Te^{j\theta} = e^{-\gamma d} \tag{6}$$

where T is the amplitude and θ is the phase angle.

Applying the natural logarithm in both sides of Equation (6), we obtain:

$$\gamma = -\frac{1}{d}ln(T) - j\frac{l}{d}(\theta + 2\pi k) = \alpha + j\beta \tag{7}$$

where $k = 0, \pm 1, \pm 2, ...$

Equation (7) allows us to obtain the propagation constant from measurements of the complex transmission coefficient. The term on the right of Equation (5) can be divided into real and imaginary parts, as shown by Equations (8) and (9). Then, we can solve for ε' and ε'', as shown by Equations (10) and (11).

$$\alpha = \frac{2\pi}{\lambda_0}\left\{\frac{\varepsilon'}{2}\left[\left(1+\frac{\varepsilon''^2}{\varepsilon'^2}\right)^{1/2}-1\right]\right\}^{1/2} \tag{8}$$

$$\beta = \frac{2\pi}{\lambda_0}\left\{\frac{\varepsilon'}{2}\left[\left(1+\frac{\varepsilon''^2}{\varepsilon'^2}\right)^{1/2}+1\right]\right\}^{1/2} \tag{9}$$

$$\varepsilon' = \left(\frac{\lambda_0}{2\pi}\right)^2\left(\alpha^2+\beta^2\right) \tag{10}$$

$$\varepsilon'' = \varepsilon'\left\{\left[\frac{2}{\varepsilon'}\left(\frac{\lambda_0\alpha}{2\pi}\right)^2+1\right]^2-1\right\}^{1/2} \tag{11}$$

By measuring the transmission coefficient τ, calculating propagation constant γ from Equation (7), and substituting in Equations (10) and (11), the complex permittivity ε^* is obtained.

Experimental realization of measurement systems

a) Coaxial probe

Several probes were manufactured using inexpensive type-N and SMA coaxial connectors and adapters. These were modified by making a cut at one of the ends to get a flat interface. The best results were obtained with SMA, which showed good frequency response and excellent repeatability. Type SMA probes made from gold plated chassis connectors are quite small; this is an advantage, for example, when testing curved samples, because contact areas appear as approximate flat.

A coaxial probe-based system is shown in Figure 3. For liquids and pulverized materials, good contact is easy to achieve by immersing the probe in the sample container; however, for the case of solid materials, a piece of rubber foam and a laboratory jack were used to improve the contact. The sample being tested is sandwiched between the probe interface and rubber foam by adjusting the jack height. The probe is connected to the test port of an 8510C vector network analyzer through a precision microwave coaxial cable.

b) Free-space

The free-space system, based on microwave transmission and reflection of waves, was set up with sets of WR-90 and WR-62 pyramidal standard gain horn antennas positioned on a rail system. VSWR of each set of antennas was measured to evaluate the extent of their frequency coverage and the similarity in their response. We found that the usable frequency range could be extended from 7 to 19 GHz using both sets.

The sample being tested was then placed between the antennas, with a fixture to hold the material sample. The distance between the antennas and the sample is set at minimum to fulfill the far field condition for the frequency range of operation of antennas:

$$\text{Distance} \geq \frac{2d^2}{\lambda}$$

where λ is the wavelength and d is the largest linear dimension of the antennas.

This ensures minimal coupling between antennas and provides a nearly flat wave front. The size of the samples sheet should be large enough to resemble a nearly infinite sample. In this case, 60×60 cm was chosen. Antennas are connected to the test ports of a vector analyzer through precision microwave cables, as shown in Figure 4.
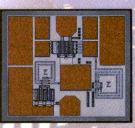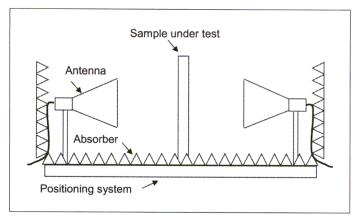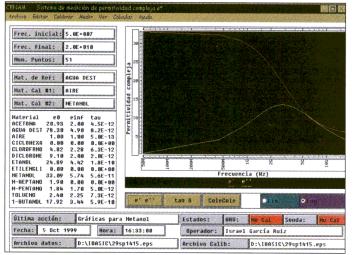
▲ **Figure 4. Permittivity measurement based on standard gain horn antennas.**

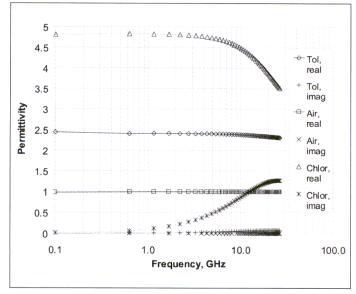▲ **Figure 5. Measurement program screen for ε^*.**

▲ **Figure 6. Real and imaginary parts of permittivity for chosen reference materials: toluene (tol), air and chloroform (chlor.).**

To automate data capturing and processing of both permittivity measurement systems, a software program was written in BASIC; the measurement program screen is shown in Figure 5.

Measurement calibration and material characterization results

The coaxial probe measurement system has to be calibrated using reference standards as required by Equation (2). Chloroform, air and toluene were chosen as suitable references. Their permittivities are known, all three are available with high purity, are easy to remove (which avoids probe contamination) and have permittivities of the same order as the expected values for those materials to be tested. Thus, the measured permittivity accuracy is improved, especially for the imaginary part, which is very small in low-loss materials. Permittivities for these reference materials are shown in Figure 6. These plots were generated using the Debye dielectric relaxation model [1], and the permittivity values to solve the equation of the model were taken from [1, 14]. A permittivity of $\varepsilon^* = 1 + j0$ has been assigned to air.

After measuring the reference materials and calculating the calibration constants A and B of Equation (6), error correction should be done at the probe interface. No prior or further calibration is needed. Tests performed by running a prior VNA traditional calibration showed no improvement in the final calculated permittivity values.

Preparation of solid samples for testing requires only a flat surface for mating with the probe interface. Samples of Teflon PTFE and Rexolite 4422 were prepared in $2 \times 2 \times 1$ cm dices, and a flat surface of 2×2 cm was polished. Surface finish tests, performed by a dimensional metrology laboratory, showed typical average roughness of $R_a = 1$ μm (see Figure 7).

Preliminary tests performed on the Teflon PTFE samples showed that a nearly flat dielectric response was obtained for the 500 MHz to 20 GHz range, with a mean value of $\varepsilon' = 2.0$ and the loss factor increasing with frequency. The 2.0 value represents a 5 percent difference compared to the well-known value of 2.1. We identified that the source of this difference could be incorrect permittivity values in one or more reference materials and/or inadequate contact at probe interface. After some testing, we found that the calibration routine needed to be modified and a solid reference material needed to be included. Although almost perfect contact is achieved with liquids, a solid surface can present imperfections, such as roughness and waviness, which have to be taken into account.
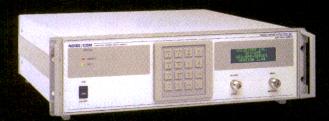
Toluene was replaced as reference material by a solid. When making tests on Rexolite we used Teflon ($\varepsilon' = 2.1$) as reference. For testing Teflon, we used Rexolite ($\varepsilon' = 2.53$) as reference. After performing the new calibration
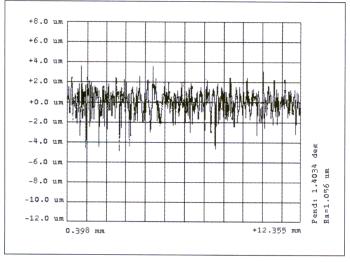
▲ **Figure 7. Typical roughness profile of samples under test.**
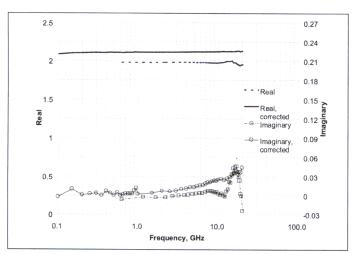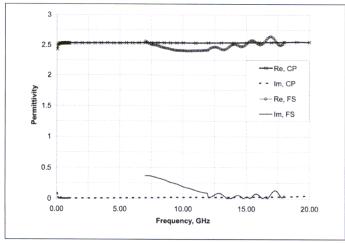

▲ **Figure 8. Permittivity of Teflon® PTFE, measured with the coaxial probe system.**

▲ **Figure 9. Permittivity of Rexolite 4422 measured with coaxial probe and free-space systems, CP: coaxial probe, FS: free-space.**

routine, samples were measured again and the results represented a substantial improvement. Figure 8 shows real and imaginary parts of permittivity of Teflon PTFE for both conditions; the dielectric response is even smoother, and the value for PTFE is closer to 2.1.

Similar results were obtained for Rexolite 4422. We also measured this material using the free-space system, which does not require the use of any reference material. Figure 9 shows permittivity values obtained with both systems, coaxial probe and free-space. Measured values closely match those reported, as obtained through other techniques [1]. The coaxial probe system allows the entire response to be obtained in a single run, with typical measurement times of about one minute. In the free-space system, it is necessary to switch the sets of antennas and recalibrate the system, which does not require the use of reference materials. Accuracy depends on the calibration of the vector network analyzer, the free-space propagation condition approximation and the dimensional accuracy of sample and positioning system.

Conclusions

Two systems for measuring complex permittivity in the microwave frequency range were developed, tested and compared. A system based on a coaxial probe allows obtaining the dielectric properties of materials in a wide band very quickly, though it depends on the use of reference materials with known permittivities for system calibration. A free-space system, based on the use of standard gain pyramidal horn antennas, is an absolute measurement system that does not require the use of any reference material; it also allows comparing results obtained using other measurement methods and covers the range from 8 to 18 GHz. Several materials were tested; dielectric characteristics for Teflon PTFE and Rexolite 4422 were obtained and compared. A good agreement between results obtained from both measurements was shown.

Coaxial probe has been widely used mostly for testing liquids and powders; however, this technique is also suitable for testing solid materials. Good contact at the probe interface is provided. Probe calibration is also important for accurate results and suitable reference materials have to be chosen.

For example, the permittivity of the reference materials should be of the same order as those for the expected values for materials under test; this consideration improves measurement of imaginary part of permittivity, which is near zero for low loss materials. Errors introduced by imperfect contact of the probe with the material under test were corrected to some degree by using one solid material in the set of references.

The free-space system allows obtaining the complex permittivity of sheets of materials for the 8 to 18 GHz. For this system, no reference materials of known permittivity are needed, there is no contact between sample

under test and measurement system and waves penetrate the whole material, providing a bulk permittivity evaluation. Comparison of results for Rexolite 4422 samples obtained with both systems shows that there is a good agreement between them, as well as with those obtained using other techniques. ∎

References

1. Arthur Von Hippel, *Dielectric Materials and Applications*, Boston: Artech House, 1995.

2. H.E. Bussey, "Measurement of RF Properties of Materials, A Survey," *Proceedings of the IEEE*, Vol. 55, June 1967: 1046-1053.

3. K. Fenske and D. Misra, "Dielectric Materials at Microwave Frequencies," *Applied Microwave and Wireless*, Vol. 12, No. 10, October 2000: 92-100.

4. J. Baker-Jarvis, M.D. Janezic, P.D. Domich and R.G. Geyer, "Analysis of an Open-Ended Coaxial Probe with Lift-off for Non-destructive Testing," *IEEE Transactions on Instruments & Measurements,* Vol 43, No. 5, October 1994: 711-718.

5. S. Jenkins, T.E. Hodgett, R.N. Clarke, A.W. Preece, "Dielectric Measurements on Reference Liquids using Automatic Network Analyzers and Calculable Geometries," *Measurement Science & Technology*, Vol. 1, 1990: 691-702.

6. C. Lin and K. Chen, "Determination of Electromagnetic Properties of Materials Using Flanged Open-ended Coaxial Probe Full Wave Analysis," *IEEE Transactions on Instruments & Measurements,* Vol. 44, 1995: 19-27.

7. D. Misra, "On the Measurement of the Complex Permittivity of Materials by an Open-ended Coaxial Probe," *IEEE Microwave and Guided Wave Letters*, Vol. 5, 1995: 161-163.

8. D.Berube and F. Gannouchi. "A Comparative Study of Four Open-ended Probe Models for Permittivity Measurements of Lossy Dielectric/-Biological Materials at Microwave Frequencies," *IEEE Transactions on MTT*, Vol. 44, 1996: 1928-1934.

9. M. Arai, J.G.P. Binner and T.E. Cross, "Estimating Errors Due to Sample Surface Roughness in Microwave Complex Permittivity Measurements Obtained Using a Coaxial Probe," *Electron Letters*, Vol. 31, 1995: 115-117.

10. R.H. Cole, J.G. Berberian, S. Mashimo, G. Chryssikos and A. Burns, "Time Domain Reflection Methods for Dielectric Measurements to 10 GHz," *Journal of Applied Physics*, Vol. 66, July 1989: 793-802.

11. D.K. Ghodgaonkar, V.V. Varadan and V.K. Varadan. "Free-space Measurement of Complex Permittivity and Complex Permeability of Magnetic Materials at Microwave Frequencies," *IEEE Transactions on Instruments & Measurements*, Vol. 39, 1990: 387-394.

12. G.F. Engen. "Microwave Circuit Theory and Foundations of Microwave Metrology," *IEE Electrical Measurements,* Series 9, Peter Peregrinus Ltd., England, 1992.

13. S. Trabelsi, A. Kraszewsky and S. O. Nelson. "Nondestructive Microwave Characterization for Determining the Bulk Density and Moisture Content of Shelled Corn," *Measurement Science & Technology*, Vol. 9, 1998: 1548-1556.

14. K. Folger, T. Friss, J. Hilland and T. Tjomsland, "A Broadband and High Sensitivity Dielectric Spectroscopy Measurement System for Quality Determination of Low-Permittivity Fluids," *Measurement Science & Technology*, Vol. 6, 1995: 995-1008.

Author Information

Israel Garcia-Ruiz received his master's degree from the Research and Advanced Studies Center of IPN in Mexico City, Mexico. He is currently pursuing his Ph.D. degree, working on techniques for material characterization using RF and microwave energy. He is employed as a microwave metrologist with CENAM, the National Measurements Institute of Mexico, where he has collaborated on the establishment of the high frequency measurement capabilities for the past eight years. He has co-authored several technical papers, as well as presentations for conferences. He may be reached by E-mail: igarcia@cenam.mx; Tel: + 52-4-2110500; or Fax: + 52-4-2110548.

Carlos David Aviles-Castro received his Ph.D. in instrumentation and measurements from the Bordeaux I University in France. Since 1992, he has been employed at CENAM; from 1992 to 1999, he headed the Electromagnetic Measurements Division; and since 1999, he has served as the research project leader in the same division. He is currently working on high accuracy electrical measurements, particularly in the Josephson effect, permittivity measurements and moisture measurements based on microwaves. He may be reached by E-mail: caviles@cenam.mx; Tel: + 52-4-2110541; or Fax: + 52-4-2110548.

Hildeberto Jardon-Aguilar received a bachelor's degree from the ESIME of the Polytechnic Institute of Mexico and a Ph.D. from Moscow Technical University of Communications and Informatics. He is employed as a full-time professor at the Research and Advanced Studies Center of IPN. He is author of more than 100 technical papers, as well as four books. He may be reached by E-mail: hjardon@enigma.red.cinvestav.mx; Tel:+52-5-7473779; or Fax: +52-5-7473880.

Products

Test software

P & H Technology Consultants has launched SoftPlot 3.0, a Windows® application for RF and microwave engineers that can capture test equipment measurement data using integral GPIB drivers.
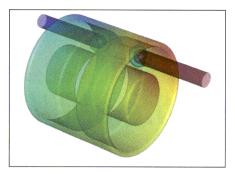
Version 3.0 adds new capability, enhances the feature set and expands the range of instruments supported. SoftPlot 3.0 introduces a serial port emulation mode that makes it possible to capture data from instruments which only have a serial port.

P & H Technology Consultants
Circle #151

Modules for test systems

Keithley Instruments offers two new software modules for its automated parametric test (APT) Systems. As add-ons for the wafer characterization software, the Keithley Test Environment (KTE), Keithley Recipe Manager (KRM) and Probe Card Manager (PCM) provide greater efficiency for production program management and productivity. The modules increase tester utilization by minimizing the potential for operator errors and provide correlation between test program changes, process control anomalies and product field failures. Keithley's KRM and PCM software modules for KTW 4.2 and higher are now available. KRM is priced at $12,500; the PCM module is priced at $10,000. Site licenses are also available.

Keithley Instruments, Inc.
Circle #152

Simulation software

COMSOL has released FEMLAB 2.1, a finite element package that serves as a tool for simulations of physical phenomena in science and technology in 1D, 2D and 3D. The solver adds a numerical method for the computation of problems where components of the solution vary on different time scales. Other features include associative geometrics in the 3D solid modeler and visualization capabilities such as transparency, which allows the user to see through surfaces. A single-user license of FEMLAB for Windows is priced at $3,995.

COMSOL, Inc.
Circle #153

Low-noise amplifier family

Intarsia has introduced the first four products in a family of low-noise amplifier (LNA) modules offering high integration levels and noise figure performance. The LNAs span the 800 MHz to 6.0 GHz frequency range and are targeted for broadband wireless access equipment, cellular base stations and infrastructure equipment for emerging wireless LAN, 802.11a, 802.11b and Bluetooth™. With noise figure performance as low as 0.65 dB, the modules serve as complete drop-in solutions requiring no external components. Samples are available now, with production quantities shipping in September. The LNAs are priced from $2 to $3 in quantities of 10,000 or more.

Intarsia Corporation
Circle #154

Tuning varactor diode

Alpha Industries has introduced the company's latest silicon hyper-abrupt junction varactor diode specifically designed for 3-volt platforms. The SMV1763-079 features a high capa-citance ratio at low reverse voltage, making it ideal for low phase noise VCOs in wireless systems up to and beyond 2.5 GHz. The tuning vacactor is designed for high-volume, low-cost battery

applications, such as low noise and wideband UHF and VHF VCO for WCDMA, GSM, PCS and analog phones. Manufac-tured in the ultra small SC-79 package and available in tape and reel, the SMV1763-079 is priced at $0.21 each for quantities of 100,000 or more.
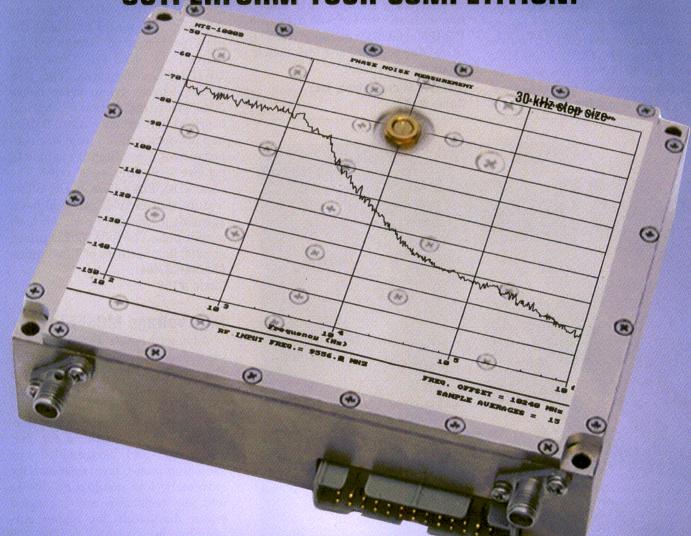
Alpha Industries, Inc.
Circle #155

Tri-mode LNA/mixer

RF Micro Devices has announced the the RF2489 LNA/mixer, a complete dual band, tri-mode receiver front end for the CDMA handset market. The RF2489 contains two LNAs, three mixers, LO divider circuitry and LO buffer outputs. It also features 30 dB of stepped LNA/mixer gain control, as well as adjustable LNA IIP3 versus bias current. Typical performance for the RF2489 for cellular LNA are 15 dB gain, 1.1 dB noise figure and +12.0 dBm IIP3; for PCS LNA, 16 dB gain, 1.3 dB noise figure and +10 dBm IIP3; and for GPS LNA, 18 dB gain, 1.2 dB noise figure and –4 dBm IIP3. The unit is priced at $2.31 in quantities of 100,000.
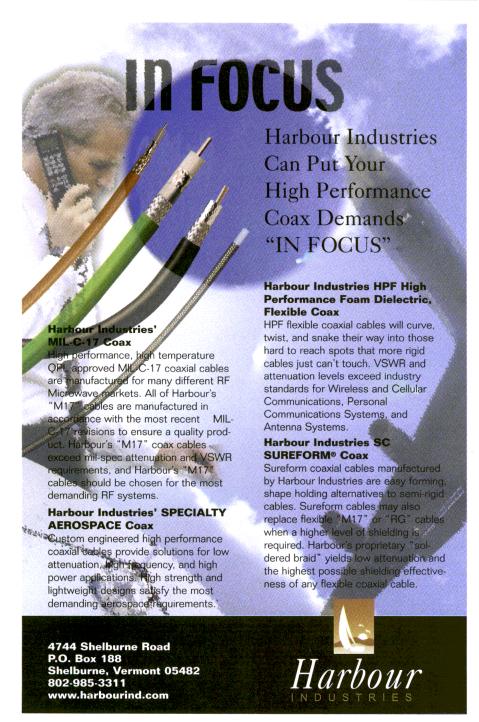
RF Micro Devices, Inc.
Circle #156

Products

Gain block amplifier

Stanford Microdevices has expanded its line of silicon germanium (SiGe) gain blocks with the introduction of the SGA-7489, designed for a range of wireless infrastructure and CATV requirements across the DC to 3000 MHz band. The SGA-7489 provides circuit designers with an easy-to-use gain block featuring high output IP3 (+36 dBm at 850 MHz), high gain (22 dB at 850 MHz) and a noise figure of 2.9 dB from a single positive supply voltage. The unit is also a suitable choice for a IF amplifier, with an OIP3 of +38 dBm and P1dB of +23 dBm at 100 MHz. The SGA-7489 is priced at $1.95 each in quantities of 10,000.

Stanford Microdevices, Inc.
Circle #157

Transimpedance amplifier

ANADIGICS has announced a new multifeature transimpedance amplifier (TIA). The second in a series of InGaP HBT TIAs, the ATA7602 is designed to deliver the high performance demanded by SONET OC-192 (10 Gb/s) and DWDM fiber networks. The new device delivers group delay below 50ps, features extended optical overload performance up to 0 dBm and provides a differential transimpedance of more than 2 kilohms to achieve –19 dBm sensitivity. The –5.2 VDC TIA offers a DC offset feature that enables external management of the duty cycle on both output pins. The ATA7602 is priced at $200 in quantities of 1,000 units.

ANADIGICS, Inc.
Circle #158
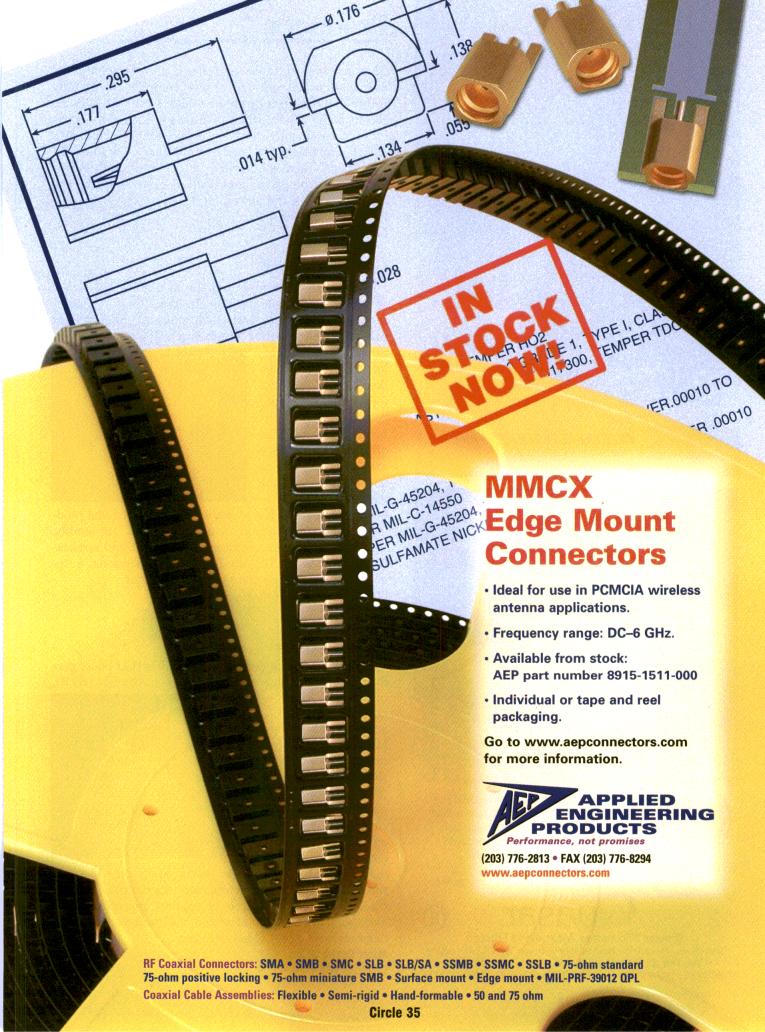
High voltage MOSFETs

Advanced Power Technology has expanded its recently introduced Power MOS 7™ product line to include 200 and 1000-volt MOSFETs. Features and benefits include low gate charge and internal chip gate resistance for fast switching and extremely low switching losses, low resistance for extremely low conduction losses and low resistance and increased power dissipation for higher current handling capability. The 200 and 1000-volt MOSFETs are priced from $8.83 to $39.17 per quantities of 1,000, depending on the current rating and package.

Advanced Power Technology, Inc.
Circle #159

Radio chipsets

Raytheon's RF Components Division is introducing a line of fully integrated radio chipsets for point-to-point, point-to-multipoint and LMDS applications at 23, 26 and 38 GHz. The chipsets are designed to be used in wireless radios and serve as alternatives to optical fiber installations for high-speed data transmission links.

Products
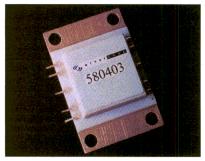
They are also suitable for cellular and personal communications networks. All chipset components are fully integrated within a common design framework, using Raytheon's 0.25 um PHEMT process. Each chipset has its own specifically designed components, including a power amplifier, low noise amplifiers, low noise/IF amplifiers, mixers, drivers, multipliers and buffer amplifiers. The component section is governed by the specifications of the power amplifier.

Raytheon Company
Circle #160

Leaded package

StratEdge has announced the availability of a new 26 to 31 GHz leaded package designed for easy manufacturing of devices with high thermal management needs, such as power amplifiers. The new product, StratEdge part number 580403, is the first leaded product for commercial applications that performs Ka-Band. This off-the-shelf package makes it possible to obtain a device in the 26 to 31 GHz frequency range that has already been packaged and readied for conventional soldering and assembly. Applications for the package include Ka-Band applications, such as LMDS, satellite communications, automotive radar and point-to-point/multipoint.

StratEdge
Circle #161

Decoder chips

Mitel has announced two decoder ICs that boost performance in satellite and terrestrial set-top box (STB), integrated television sets and PC applications. The MT312 for satellite applications and the MT351 for terrestrial receivers provide auto-scan capability, which enables systems to detect and tune digital television channels delivered by satellite and terrestrial links. The devices also incorporate the digital functionality required to support interactive services such as two-way television, e-commerce, video-on-demand and digital video encoding.

Mitel Corporation
Circle #162

Products

Broadcast devices

A family of RF power MOSFETs using Motorola's RF LDMOS technology is now available for broadcast transmitter equipment. The MFR370 series is designed to cover the frequency spectrum of 470 to 860 MHz (bands IV/V) used for TV transmission worldwide. The first product to be introduced is the MRF372, an internally matched, 180-watt, 32-volt lateral N-channel broadband RF power MOSFET. It is designed for broadband commercial and industrial applications at frequencies from 470 to 860 MHz. The high gain and broadband performance of this device makes it ideal for large-signal, common source amplifier applications in 32-volt transmitter equipment. The suggested resale price is $100 each in 10,000-piece quantities.
Motorola, Inc.
Circle #163

Integrated circuit receiver

Mimix Broadband introduces a totally integrated gallium arsenide (GaAs) monolithic microwave-integrated circuit (MMIC) receiver on a single chip. The XR1000 is a three-stage low-noise amplifier (LNA) followed by an image reject fundamental mixer, with Lange couplers included to improve bandwidth. Using 0.15 micron gate length GaAs pHEMT, the receiver covers the 17 to 27 GHz frequency band. The XR1000 has a typical small-signal conversion gain of 10 dB, with typical noise figure of 3.5 dB and 15 dB typical image rejection across the band.
Mimix Broadband, Inc.
Circle #164

Power management ICs

Fujitsu Microelectronics has introduced to the North American market three power management integrated circuits (ICs) designed for cellular phones, personal digital assistants and other mobile devices. The new devices fulfill the requirements of digital systems such as CDMA, GSM and W-CDMA. The new set of power management devices includes the MB3891, which was developed specifically for current and future GSM applications and future W-CDMA applications. Another model, the MB3892, includes 12 LDOs, reset control, Lithium-ion (Li) battery charger, receiver and speaker amplifiers, serial interface, 4-channel D/A converter, LED drivers and temperature protection function. Pricing for these ICs starts at $2.75 each in quantities of 1 million or more.
Fujitsu Microelectronics, Inc.
Circle #165

Products

PLL integrated circuits

Peregrine Semiconductor has introduced two new products targeted for cellular and PCS base stations: LMDS and MMDS broadband wireless access systems, wireless loop systems and terrestrial satellite systems. The PE3339 and PE3340 are Integer-N PLLs uniquely capable of frequency synthesis up to 3.0 GHz. Hence, an external prescaler is not required to operate these phase-locked loop (PLL) ICs for many applications where the desired local oscillator (LO) is between 2.2 and 3.0 GHz. The PLL ICs are built using Peregrine's ultra-thin-silicon (UTSi) silicon-on-sapphire (SOS) CMOS process.
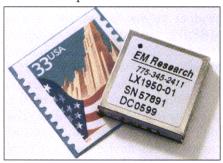
Peregrine Semiconductor
Circle #166

Frequency synthesizer

EM Research offers LX-Series surface-mount frequency synthesizers, which are custom-designed for broadband mixer LO applications. This product features fixed-

frequency or programmable outputs in bands from 50 to 2700 MHz, with up to octave bandwidths (at f_c ≤600 MHz). At 1 GHz frequency output, phase noise characteristics are –98 dBc/Hz at 10 KHz offset and –120 dBc/Hz at 100 KHz offset. Packaged in a 0.75-inch-square surface-mount housing, the LX-Series frequency synthesizer is suited for use in broadband wireless communications systems.
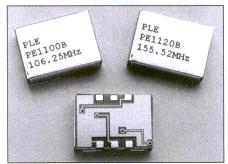
EM Research, Inc.
Circle #167

Tight spec oscillators

Pletronics has announced a line of differential PECL output oscillators, with available frequencies ranging from 10.0 to 170.0 MHz. The PE1100BV series uses a true crystal design for ultra low jitter (3 pS RMS maximum for >70.0 MHz). The parts have an input voltage (V_{cc}) of 3.3 volts ±10 percent or 5 volts ±10 percent. Standard frequency stabilities are ±20 PPM,
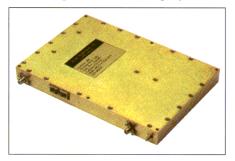
Products

±25 PPM and ±50 PPM over the operating temperature range of 0 to 80 degrees Celsius. Standard symmetry is 45/55. Depending on specs and quantity, pricing starts at $13.
Pletronics, Inc.
Circle #168

Frequency synthesizers

The MFS series of low-power microwave frequency synthesizers from Elcom Technologies consumes only 8 watts of power, making it ideal for applications requiring wider operating temperatures for use alongside small power supplies. The compact devices employ a single module design implemented with CMOS ASICs, advanced MMICs and a microprocessor. A KU-band synthesizer with 1 kHz step, 2.2 GHz bandwidth and integrated L-band LFLO consumes only 8 watts. Ruggedized and field tested for operation over a wide temperature, shock and vibration range, the synthesizers meet the requirements of IESS 308, Eutelsat and MIL-STD188-146.
Elcom Technologies, Inc.
Circle #169

Surface mount oscillators

Rakon has introduced two ultra miniature TCXOs. These tiny surface mount oscillators have footprints of 7 × 5 mm and 5 × 3 mm. The oscillators are available with ±1 ppm frequency stability, a frequency range from 10 to 26 MHz, are screened for perturbations and have high-quality stability, shock and vibration performance to optimize the performance and quality of all wireless products. Wireless applications include Bluetooth, 3G, GPRS and Edge cellular phones, wireless modems, two-way pagers, microwave wireless, GPS and many wireless applications.
Rakon
Circle #170

SAW-based oscillators

Micro Networks has developed a series of voltage-controlled SAW oscillators (VCSOs) that are ideal for high-performance telecommunication applications. The M600 series of VCSOs utilize Micro Networks' capability in the design of high-performance oscillators featuring low phase noise and jitter over a frequency range of 300 to 900 MHz. These devices are suited for phase-locked loop applications, as well as clock and date recovery and clock smoothing circuits used

Products

in OC-12, OC-48 and OC-192 SONET/SDH systems. The M600 series is available in a 28-pin surface mount package and offers an output disable feature that forces the output into a static condition, enabling an external clock to control the output frequency. Operating from a single +5-volt supply, the M600's differential outputs are 10K/100K PECL logic compatible.

Micro Networks
Circle #171

Clock oscillator

Temex Components has announced the availability of the new Rubidium atomic clock, the MCFRS series, that consumes less than 6.0 amps during a warm-up

time of 10 at 25 degrees Celsius. The products are available in the standard frequencies of 5, 10 and 20 MHz. The MCFRS consumes only 8 watts of power and exhibits low aging of $\pm 4 \times 10^{-11}$/month. The MCFRS input voltage is 22 to 28 volts and is connected through a 10-pin sub-D with a female coaxial contact. There is an RS-232 port interface for center frequency adjustment and monitoring of the working parameters. It can be mounted vertically or horizontally and operates in a temperature range of –0 to +60 degrees Celsius. An extended temperature range version of –20 to +65 degrees Celsius is also available.

Temex Electronics, Inc.
Circle #172

Tracking filter/oscillator

Omniyig has introduced its new Model M120YTO, a multioctave

tracking YIG filter with YIG oscillator. The filter covers a frequency range of 2.0 to 8.0 GHz, with the oscillator offsetting by 160 MHz above the filter. The RF power output is +13 dBm minimum, with FM noise at –120 dBc at 100 kHz away. The unit is built to Mil-E-5400 specification andscan be integrated with an analog driver or 12-bit digital driver to tune the full frequency range. Operating temperature range is –54 to +85 degrees Celsuis.

Omniyig, Inc.
Circle #173
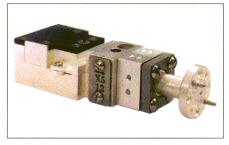
Voltage-controlled SAW oscillator

Sawtek introduces two voltage-controlled SAW oscillator (VCSO) products for most broadband access applications. The single-ended sine wave VCSO features frequencies from 300 MHz to 2.5 GHz, with 622.08 MHz, 666.51 MHz and 2.488 GHz being standard frequencies. It provides surface transverse wave (STW) resonator technology, offering low phase noise and extremely low noise floors to ensure high frequency jitter performance (<5 fs RMS), and low g-sensitivity versions at up to 5×10^{-10}/g. The differential ECL clock VCSO features frequencies from 600 MHz to just over 1 GHz, with standard frequencies at 622.08 and 666.51 MHz, and STW resonator technology offering low jitter performance at high fundamental frequencies (<.3 ps RMS). Both are designed for use in phase-locked loop applications.

Sawtek
Circle #174

Active multipliers

Gilland Electronics' ELVA-1 Division has introduced the IAFM-series millimeter active multipliers, which produce up to 25× frequency multiplication in a single stage, using a C-band input source. IAFMs can accept up to 600 milliwatts of input power with no ill effects. They are designed for reliability under harsh conditions, with an operating temperature range of

–50 to +70 degrees Celsuis and an estimated MTTF of 50,000 hours. Specifications common to all models are 3 dB maximum power deviation within a 1 percent bandwidth, a minimum of 40 dB of adjacent harmonics rejection, VSWR of 1.3:1 and maximum AM noise insertion of –130 dB/Hz (white noise). Applications for IAFMs include electronically tuned power sources, frequency synthesizers, digital radios, spectroscopy or radiometry.

Gilland Electronics, Inc.
Circle #175

Tuning oscillator

Mini-Circuits has introduced the ROS-150, a compact, voltage-controlled oscillator providing 75 to 150 MHz octave band tuning, low –103 dBc/Hz SSB phase noise typical at 10 kHz offset and –23 dBc (typical) harmonic suppression.
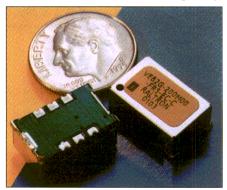
Products

With 9.5 dBm typical power output, this miniature 12-volt, 20 mA (maximum current) VCO measures only 0.5 × 0.5 × 0.18 inches and is ideal for test instruments, such as signal generators. Operating temperature range is –55 to +85 (max.) degrees Celsius. The 5 to 49 unit low quantity price is $12.95 each.

Mini-Circuits
Circle #176

Voltage-controlled crystal oscillator

Raltron Electronics has announced a new 200 MHz VCXO that reduces system-accumulated jitter and noise. The new VC-8000 VCXO uses an inverted-mesa quartz crystal to combine higher frequency, lower noise, increased stability, wider pullability range

and faster on/off times. The VC-8000 provides a voltage-controlled reference output frequency up to 200 MHz, with less than 1 picosecond jitter and an overall frequency

stability of ±30 ppm. Units are available at any desired output frequency from 65 to 200 MHz. Long-term stability is specified at ±2 ppm per year and pullability at ±100 ppm. The VC-8000 operates from either 3.3- or 5-volt rails, and the operating temperature range is 0 to +70 degrees Celsius. The VC-8000 VCXOs are priced from $39 to $49 each in OEM quantities of 10,000 units, depending on frequency and options.

Raltron Electronics Corporation
Circle #177

SIGNAL PROCESSING

AIN termination

Bird Component Products continues to add environmentally friendly products to its line of terminations. The Model 100-NST-FN uses aluminum nitride as an alternative to BeO substrates. The unit has a frequency range of DC-3 GHz and VSWR DC-1 GHz at 1.1:1 maximum; 1 to 3 GHz at 1.15:1 maximum. The power rating is 100 watts average and connectors available are BNC, N, TNC and 7/16.

Bird Component Products, Inc.
Circle #178
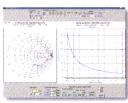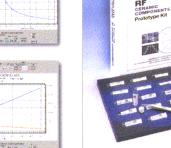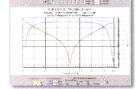
Products
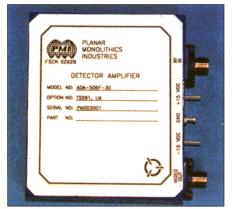
Bandpass filter

Microwave Filter has introduced the Model 14042 bandpass filter, which is used to prevent PCS interference at the ENG receive site. It passes the entire ENG band (channels 1 through 10, 1990 to 2500 MHz). The unit provides stopband rejection of 25 dB (minimum) at 1910 MHz and 2580 MHz, with a

bandpass insertion loss of 1.0 dB (maximum). The impedance is 50 ohms, with standard "N" (female) connectors. It is designed for indoor use, but can be provided as a temperature compensated unit. The size is $6 \times 2 \times 2$ inches.

Microwave Filter Company
Circle #179

Linear amplifier detector module

Planar Monolithics produces a variety of amplifier products that operate up to 20 GHz. The new Model ADA-506F-TSS61-LM is a DC-coupled, temperature-compensated, linear amplifier detector module with 30 dB of dynamic range. The module operates from 5.4 to 5.9 GHz, with an 8 ns rise time and a 10 ns fall time (0.5 to 20.0 GHz units are available). This unit operates on +15 VDC at 20 mA and –15 VDC at 80 mA and measures $2.5 \times 2.9 \times 0.5$ inches.

Planar Monolithics Industries, Inc.
Circle #180

Electronically tunable RF delay line

Paratek Microwave has introduced an electronically tunable RF delay line. Features include software-controlled delay tunability (up to 30 percent of fixed delay), low insertion loss, low power consumption and compact size. Benefits include reduced system assembly and test time, and enabling electronic compensation for aging effects in power amplifiers, with the application being feed-forward power amplifiers. Specifications include a frequency of 1750 to 1900 MHz, a time delay range of 4.0 ns ±0.5 ns, an insertion loss of 4 dB, 0.5 degrees phase linearity, 19 dB return loss, 70 dB linearity (IP3) and SMA RF interface. Customized interfaces are also available.

Paratek Microwave, Inc.
Circle #181

Products

RF digitizer

IFR Systems has introduced the 2319E, the first in a series of signal analysis instruments. The 2319E is a benchtop or rack-mounted RF digitizer for 2G, 2.5G and 3G digital cellular testing. Features include conversion of RF signals to digital data for processing in a PC, GSM/EDGE and UMTS real-time demodulation application software,

500 MHz to 2.5 GHz frequency range, 50-watt input power handling, 20 MHz wide digitization bandwidth, 65.28 M samples/second sample rate, 12-bit ADC resolution, phase noise of –121 dBc/Hz, sensitivity of –153 dBm/Hz, built-in FFT spectrum monitor, 1 mega sample internal IQ data memory and optional analog IQ inputs and outputs. The 2319E RF digitizer is priced at $31,351.
IFR Systems, Inc.
Circle #182

Test system

Spirent Communications has introduced the TAS cdma2000 Interference Lab (TAS CIL) test system. The system is designed to meet the receiver testing requirements for cdma2000 wireless terminals and base stations. The TAS CIL combines the features of the TAS5600C universal interference emulator with the impairments found in the TAS4600A noise and interference emulator. The system provides co- and adjacent-channel interference and provides complete coverage of the cellular and PCS bands. Pricing starts at $89,950.
Spirent Communications
Circle #183

Harmonic tuners

Focus Microwaves offers new high accuracy harmonic tuners. These tuners offer reflection between 0.92 and 0.98 at user selectable harmonic frequencies by simple changing of resonators; fine resolution tuning accuracy is between 0.2 and 0.5 degrees over the entire 0 to 360 degree range. This is achieved through precise alignment supported by callibration and non-linear interpolation algorithms allowing reproduction of arbitrary impedances, with accuracy typically exceeding –50 dB. This system allows characterization of complex and nonlinear behavior of microwave transistors, including hot IV curves, saturation plots and load pull contours, and both have harmonic impedance pulling.
Focus Microwaves, Inc.
Circle #184

Amplifier test system

Anritsu Company has enhanced its ME7840A power amplifier test system with additional measurement capability. The system can now conduct ACPR, IMD, PAE, compression, harmonics and S-parameter measurements with a single connection, creating a turnkey solution that allows for convenience, speed and accuracy. A single-connection test set that supports 100 watt testing between 800 and 2400 MHz is at the center of the system. The test set also accom-

modates external instruments for ACPR measurements. The standard ME7840A is priced at $79,000.
Anritsu Company
Circle #185

Compact analyzer

B+K Precision has announced the Model 2635, a 150 kHz to 1.05 GHz spectrum analyzer. This compact PC compatible benchtop unit can be used for precompliance testing during development prior to

third-party testing. It is flexible and can be used to test cable TV levels and frequency responses, test master antenna TV systems, measure communications transmitter spurious radiation, locate sources of EMI or measure unwanted RF radiation. It is priced at $3,295.
B+K Precision Corporation
Circle #186

Spectrum analyzer

Morrow Technologies has introduced its P9116 Satcom spectrum analyzer, which monitors systems remotely. Users simply need to locate the P9116 analyzer at the base station and operate it remotely from any location via the Internet, LAN or modem. The P9116 includes a virtual spectrum analyzer front panel that allows users to view and control the spectrum display in real time, with no third party software or hardware required. The P9116 is a full-featured spectrum analyzer that covers the 100 kHz to 1.6 GHz frequency range. The instrument's chassis includes a complete Pentium PC and Windows NT operating system.
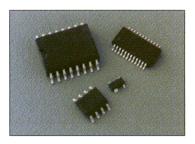**Morrow Technologies Corporation**
Circle #187

Circulator-Coupled Equalizers Applicable to High-Speed Digital Data Links
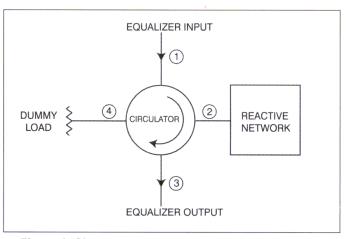
By Richard M. Kurzrok, PE
RMK Consultants

As microprocessors achieve operations above 1.5 GHz, transmission of high-speed digital data entails signal processing at microwave frequencies [1]. Microwave equalization techniques [2, 3, 4] are necessary to avoid data stream impairments due to transmission distortion.

One type of applicable equalizer uses a four-port circulator, as shown in Figure 1. The second port of the circulator is connected to a reactive network. Equalizer transmission uses an input at the first circulator port, reflection at the second circulator port, and output at the third circulator port. The fourth circulator port is terminated in a dummy load.

The ideal circulator-coupled equalizer permits adjustment of equalizer transmission responses substantially independent of the equalizer input and output return losses. In this article, the circulator-coupled equalizer will be examined as a bandpass type of group delay equalizer. Parabolic group delay distortion can be corrected by tuning the equalizer to a design center frequency. Linear group delay distortions can be corrected by adjusting the equalizer responses about points of inflection above or below the design center frequency. Circulator-coupled equalizers can also be used for amplitude equalization. [5]

Reactive networks

Reactive networks determine the equalizer responses shapes. These networks utilize nomenclature similar to bandpass filters with direct coupled resonators [6]. The reactive network for a C-Section group delay equalizer uses

▲ **Figure 1. Circulator coupled equalizer.**
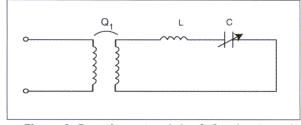
▲ **Figure 2. Reactive network for C-Section ($n = 1$) lumped circuit prototype.**

a singly loaded resonant circuit. The lumped circuit equivalent is shown in Figure 2. The equalizer bandwidth is adjusted by varying the resonator singly loaded Q and the equalizer center frequency is adjusted via a variable capacitor. The reactive network of a D-Section group delay equalizer uses two coupled resonators. The lumped circuit equivalent is shown in Figure 3. The equalizer bandwidth is adjusted by varying

▲ **Figure 3. Reactive network for D-Section (*n* = 2) lumped circuit prototype.**

the coefficient of coupling between the two synchronously tuned resonators. The equalizer shape factor is adjusted by varying the singly loaded Q of the input resonator. The resonator center frequencies are adjusted via the two variable capacitors.

Transmission line reactive networks can also be used. D-Section equalizers, using coupled comb-line resonators, at nominal 1 GHz frequencies, have been designed, fabricated, and tested for use in satellite earth station equipment. These equalizers have four mechanical controls: input coupling, interstage coupling, and two resonator tuning adjustments. Microwave couplings can be readily developed using nodal voltages [7].

Equalizer group delay responses

The normalized frequency variable x is defined per Equation (1):

$$x = 2\left(\frac{f - f_0}{\Delta f}\right) \tag{1}$$

where f = frequency
f_0 = center frequency
Δf = normalizing bandwidth

The total Q of the equalizer is defined per Equation (2):

$$Q_T = \frac{f_0}{\Delta f} \tag{2}$$

The total Q is used to denormalize any normalized circuit parameters. (Note: Normalized parameters use lower case variables and absolute parameters use upper case variables.)

The unloaded Q of the equalizer is a measure of resonator quality. It is designated as Q_0. The normalized dissipation factor d_0 is defined per Equation (3):

$$d_0 = \frac{Q_T}{Q_0} \tag{3}$$

The normalized singly loaded q of the input resonator is designated as q_1. For a C-Section (n = 1) reactive net-

work, $q_1 = 1.0$. The actual singly loaded Q for the C-Section is obtained by denormalizing per Equation (4):

$$Q_1 = q_1 Q_T \tag{4}$$

where Q_1 = absolute singly loaded Q.

All C-Section group delay responses are monotonic.

The normalized coefficient of coupling for the D-Section (n = 2) reactive network is k_{12}. The absolute coefficient of coupling K_{12} is shown in Equation (5):

$$K_{12} = \frac{k_{12}}{Q_T} \tag{5}$$

For the D-Section, there is a shape factor C as shown in Equation (6):

$$C = \frac{1}{(q_1 k_{12})} = \frac{1}{(Q_1 K_{12})} \tag{6}$$

When $C = \sqrt{3} = 1.732$, the group delay response of the lossless D-Section is maximally flat. When C is less than 1.732, the group delay is monotonic. When C is greater than 1.732, the group delay response is no longer monotonic, and group delay peaks occur above and below the equalizer center frequency.

The group delay responses are normalized. The absolute group delay responses are obtained by multiplying the normalized response by T, as shown in Equation (7):

$$T = \frac{T_0}{(\pi f_0)} \tag{7}$$

where T_0 is a constant for each different normalized group delay response.

When f_0 is in MHz, the absolute group delay will be in microseconds. When f_0 is in GHz, the absolute group delay will be in nanoseconds.

Equalizer responses

Equalizer transmission responses have been computed for several configurations. For normalized frequency range of $x = 0$ to $x = 1.1$, C-Section amplitude and normalized group delay responses for selected normalized dissipation factors are shown in Table 1. For the same normalized frequency range, D-Section amplitude and normalized group delay responses for selected normalized dissipation factors and a shape factor C = 1.732 are shown in Table 2.

X	$D_0 = 0$ L (dB)	$T_0 = 2.000$ T	$D_0 = 0.05$ L (dB)	$T_0 = 2.216$ T	$D_0 = 0.1$ L (dB)	$T_0 = 2.469$ T	$D_0 = 0.2$ L (dB)	$T_0 = 3.125$ T
0	0	1.000	0.869	1.000	1.743	1.000	3.522	1.000
0.05	0	0.998	0.867	0.997	1.739	0.997	3.512	0.996
0.1	0	0.990	0.861	0.989	1.725	0.988	3.485	0.985
0.15	0	0.978	0.850	0.976	1.704	0.973	3.439	0.966
0.2	0	0.962	0.836	0.958	1.675	0.953	3.378	0.941
0.25	0	0.941	0.818	0.935	1.639	0.928	3.302	0.911
0.3	0	0.917	0.797	0.909	1.597	0.900	3.214	0.877
0.35	0	0.891	0.774	0.880	1.550	0.869	3.116	0.839
0.4	0	0.862	0.749	0.849	1.500	0.835	3.010	0.800
0.45	0	0.832	0.722	0.817	1.446	0.800	2.899	0.760
0.5	0	0.800	0.695	0.783	1.390	0.764	2.785	0.719
0.55	0	0.768	0.667	0.749	1.334	0.728	2.669	0.679
0.6	0	0.735	0.639	0.715	1.277	0.692	2.553	0.640
0.65	0	0.703	0.611	0.681	1.221	0.657	2.438	0.602
0.7	0	0.671	0.583	0.648	1.165	0.623	2.325	0.566
0.75	0	0.640	0.556	0.616	1.111	0.590	2.215	0.532
0.8	0	0.610	0.529	0.585	1.058	0.559	2.109	0.500
0.85	0	0.581	0.504	0.555	1.007	0.529	2.006	0.470
0.9	0	0.552	0.480	0.527	0.958	0.500	1.908	0.441
0.95	0	0.526	0.456	0.500	0.912	0.473	1.815	0.415
1.0	0	0.500	0.434	0.474	0.867	0.448	1.725	0.390
1.05	0	0.476	0.413	0.450	0.825	0.424	1.641	0.367
1.1	0	0.452	0.393	0.427	0.785	0.401	1.561	0.346

▲ Table 1. Computed C-Section ($n = 1$) circulator coupled equalizer amplitude and group delay responses.

In the tables, the constant T_0 is shown for each set of responses. Arithmetic symmetry has been assumed (frequency sensitivity of couplings and other inherent asymmetries have been neglected) so that responses for minus x are identical to responses for plus x. It can be seen that equalizer amplitude responses peak at $x = 0$ when d_0 is not equal to zero. This band-reject behavior of lossy equalizers can provide useful supplementary amplitude equalization in some applications.

When D-Sections do not provide sufficient group delay correction, one or more C and D Sections can be cascaded. This requires more than one four-port circulator. A single circulator can be used with reactive networks of three or four direct coupled resonators [4]. This technique can result in some cost savings.

Circulators

Ferrite junction circulators have been commercially available for almost 40 years. The four-port circulator usually requires two ferrite junctions. Typical circulator performances are forward loss less than 0.5 dB, reverse isolation greater than 20 dB, and return loss of 20 dB. As the frequency drops to 1 GHz or below, ferrite devices usually operate above resonance and usable bandwidths become quite limited. Some circulators are capable of handling medium or high-power levels.

In recent years, the electronic circulator has become a possible alternative below 1 GHz [8]. It uses operational amplifiers. A four-port circulator requires four operational amplifiers with various passive components. Each amplifier stage has a voltage gain of 3.236. Resistor values are directly related to the prevailing circulator impedance level. Capacitors are used for bypassing at the DC busses. Dynamic range of the electronic circulators is limited by the operational amplifiers. The electronic circulator is currently not available from commercial vendors.

Equalizer integration

The electronic circulator can achieve the first level of integration using an operational amplifier quad. An application specific integrated circuit (ASIC) could include the quad operational amplifier and all passive components. Large scale integration would include the electronic four port circulator and the reactive network. Equalizer adjustments in the reactive network could be realized electronically using varactors in the resonators and the couplings. A fully integrated equalizer could ultimately be included in complete integration at the systems level.

Future equalizer integration would ordinarily be preceeded by a market survey and standardization of digital data transmission requirements.

Conclusion

The circulator-coupled group delay equalizer can be a useful unit for high quality digital data links at microwave frequencies.

www.werlatone.com

Directional Couplers | Combiners | Dividers | 90°/180° Hybrids

WERLATONE | SINCE 1965

X	D₀ = 0	T₀ = 3.464	D₀ = 0.05	T₀ = 4.173	D₀ = 0.1	T₀ = 5.169	D₀ = 0.2	T₀ = 8.757
	L (dB)	T	L (dB)	T	L (dB)	T	L (dB)	T
0	0	1.000	1.508	1.000	3.039	1.000	6.277	1.000
0.05	0	1.000	1.508	1.000	3.039	1.000	6.276	1.000
0.1	0	1.000	1.508	1.000	3.309	1.000	6.273	0.998
0.15	0	1.000	1.507	0.999	3.037	0.999	6.267	0.995
0.2	0	0.998	1.506	0.998	3.033	0.996	6.254	0.990
0.25	0	0.996	1.502	0.995	3.026	0.993	6.231	0.982
0.3	0	0.993	1.497	0.991	3.013	0.986	6.195	0.970
0.35	0	0.987	1.488	0.983	2.994	0.977	6.143	0.952
0.4	0	0.978	1.475	0.973	2.966	0.964	6.071	0.930
0.45	0	0.967	1.457	0.959	2.929	0.947	5.978	0.901
0.5	0	0.952	1.435	0.942	2.882	0.926	5.861	0.867
0.55	0	0.934	1.407	0.921	2.825	0.900	5.722	0.829
0.6	0	0.913	1.375	0.896	2.757	0.870	5.562	0.786
0.65	0	0.889	1.337	0.867	2.679	0.837	5.384	0.740
0.7	0	0.861	1.296	0.836	2.594	0.801	5.190	0.693
0.75	0	0.832	1.251	0.803	2.501	0.763	4.985	0.646
0.8	0	0.800	1.203	0.767	2.404	0.724	4.773	0.599
0.85	0	0.767	1.154	0.731	2.303	0.684	4.556	0.554
0.9	0	0.734	1.103	0.695	2.200	0.645	4.339	0.511
0.95	0	0.700	1.052	0.659	2.097	0.607	4.125	0.471
1.0	0	0.667	1.002	0.623	1.995	0.570	3.915	0.434
1.05	0	0.634	0.952	0.589	1.895	0.534	3.711	0.400
1.1	0	0.602	0.903	0.555	1.797	0.500	3.515	0.369

▲ **Table 2. Computed D-Section (n = 2) circulator coupled equalizer amplitude and group delay responses for shape factor = 1.732.**

At some of the lower microwave frequencies, ferrite circulators can be replaced by electronic circulators at receive signal levels. This provides an alternate design approach with wider bandwidths than ferrite circulators. Future designs of integrated circuit equalizers can achieve new levels of miniaturization and cost reduction. ■

References

1. G.A. Breed. "New Digital Technologies Look a Lot Like Microwaves," *Applied Microwave & Wireless*, July 1999: 10.

2. J.O. Scanlon and J.D. Rhodes. "Microwave All-Pass Networks-Part I," *IEEE Transactions on Microwave Theory and Techniques*, Vol. MTT-16, February 1968: 62-79.

3. E.G. Cristal. "Theory and Design of Microwave All-Pass Equalizers," *IEEE Transactions on Microwave Theory and Techniques*, Vol. MTT-17, January 1969: 28-38.

4. R.M. Kurzrok. "Microwave Phase Equalizers," *Frequency Technology*, May 1970: 16-19.

5. R.M. Kurzrok. "Amplitude Equalizer is Circulator Coupled," *Microwaves*, September 1971: 50-52.

6. M. Dishal. "Dissipative Band-Pass Filters," *Proc. of IRE*, Vol. 37, September 1949: 1050-1069.

7. R.M. Kurzrok. "Nodal Voltages Offer Key to Filter Design," *Microwaves & RF*, April 1999: 72-84 and May 1999: 67-69.

8. C. Wenzel. "Low Frequency Circulator/Isolator Uses No Ferrite or Magnet," *RF Design*, July 1991.

Author information

Richard M. Kurzrok, PE, is an independent consultant specializing in filters and equalizers from baseband through microwave frequencies. He can be reached at RMK Consultants, 82-34 210th Street, Queens Village, NY, 11427-1310; Tel: 718-776-6343; Fax: 718-776-6087; and E-mail: rmkconsulting@aol.com.

System and Thermal Management Solutions for 3G Basestations

Precise temperature monitoring can be used to efficiently control fans, air conditioning and other cooling processes

By David Hanrahan
Analog Devices, Inc.

The awe-inspiring vision of mobility "anytime, anywhere" and increasing consumer demands for convergence are driving forces behind the latest challenges for system designers worldwide. No longer are we content with having the ability to speak to our families several time zones away using a cell phone or send holiday photos via e-mail that propagates continents in the blink of an eye. We want to have both 24-hour, seamless connectivity and unlimited freedom to roam the globe. The technology that promises to deliver is 3G.

The current generation of mobile phones allows us to speak, send simple text and picture messages, while WAP services allow limited text interface to Internet sites. 3G promises to enhance the experience with data rates of 2.4 megabits per second, allowing high-speed data services such as wireless Internet access and streaming video to wireless devices. The high performance and sheer complexity of both wireless terminals and cellular infrastructure alike will stretch the imaginations of systems designers and test their abilities to the limit. This article focuses on the 3G basestation design from a systems management perspective.

Challenges of 3G design

What are the challenges facing the 3G basestation designer? First, the fundamental hardware choices have to be made, when migrating from the current 2G solutions such as TDMA, CDMA or GSM to 3G solutions based around EDGE or WCDMA. This task is so great that IMT-2000 defines the evolution of 3G through intermediate technologies such as GPRS or cdma2000 1X. But no matter what technology or topology is used, one problem will be common to all systems: the generation of heat and how to dissipate it safely. The designer is faced with integrating more and more functionality into tighter form factors, to the detriment of natural airflow. The designer must architect a feature-rich solution at the lowest possible cost. The primary driver for good thermal design will be the absolute need for "high availability."
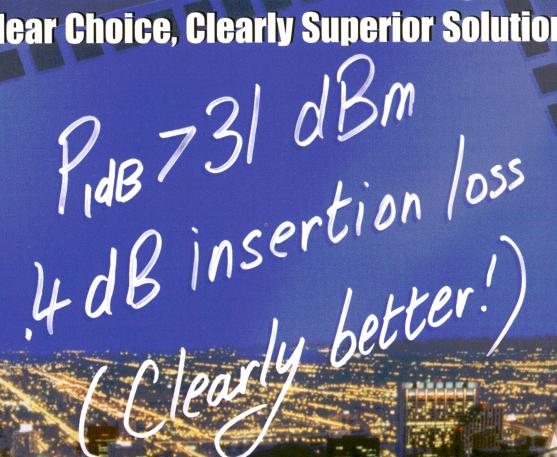
"High availability" is the industry term for systems that demand extremely high system reliability and would ideally operate 24 hours a day, seven days a week, 365 days a year. The target for a high availability system is to be up for 99.999 percent of the time. This equates to a system downtime of only five minutes a year, including planned maintenance! It is imperative in the telecommunications industry that equipment run reliably and not fail. Any communications outages will cost the service provider dearly in the form of dropped call compensation or even lost business.

Supporting corporate customers and emergency services now requires a level of dependability that in the past were synonymous with mission-critical systems as found on commercial aircraft or the space shuttle. The measures taken by the designer to ensure a highly available system should be in proportion to the impact a system failure would have on the core business. Using this approach makes for a more sensible, well-conceived design that has a greater chance of working reliably first time. Spending a few dollars up front on thermal and systems management could save potentially thousands or even millions of dollars later.

A recent survey [1] found that the most common causes of system failure were AC power problems, system hangs, disk failures, CPU

▲ Figure 1. Typical contributors of heat in a 3G basestation design.

can dissipate hundreds of watts of heat energy. Uncontrolled, this will lead to component/module overheating and, ultimately, system failure.

Figure 1 shows a system-level view of the largest heat contributors in a basestation. The greatest offender heat-wise will be the RF power amp at the front-end. Having a method of measuring the temperature of the RF power amplifier is not only essential for adequate cooling but is also desirable for controlling the power output accurately and ensuring power output stability.

The heat generated by the back-end is reflective of the amount of raw computing power harnessed and the volume of data, voice and broadband traffic handled. The core of the basestation is generally either a CPU or a dedicated DSP controller. As data rates increase and packets are processed locally, the core temperature of the system will increase and need to be measured. Many CPUs already have an embedded thermal diode to allow the processor's die temperature to be monitored.

errors and memory errors. The better a designer can manage system parameters and predict impending failure, the more reliable the system becomes, and the total cost of ownership (TCO) is reduced.

How can the designer adequately address these issues? A two-pronged approach makes for a reliable system design: identifying potential problem areas in advance, and designing a mechanism to detect impending/potential failures and report them automatically to management software.

Identifying problem areas in advance

The high demands of 3G basestation technology on data/voice throughput, compact physical size, computational power, built-in redundancy and flexibility mean that practically all areas of the design present potential component failure unless addressed. The biggest problem is heat dissipation. The industry trend is toward increased component power and component density on boards and modules, resulting in more heat dissipation per square inch of PCB than ever before. Typical sources of heat include the RF front-end, the CPU- or DSP-core, memory and network interface. The average basestation

Managing thermals

The proposed technique for measuring temperature in the basestation is thermal diode monitoring (TDM). This technique uses a transistor as the temperature-sensing element and takes advantage of the transistor's relationship between V_{BE} and temperature. Thermistors have traditionally been used to measure temperature. However, the thermistor's resistance change with temperature is a nonlinear function and so requires additional support circuitry to output valid temperature data. Thermistors also tend to have a poor response to fast temperature transients and are difficult to mount in good contact with measurement surfaces using automated pick-and-place equipment.

The advantage of using a transistor to measure temperature is that multiple devices can be placed discretely throughout the system to give a fully distributed temperature sensing solution. With some forethought, a designer can even integrate the measurement transistor directly onto the dies of the expected hottest ICs (i.e., having the silicon vendor do it). This allows the designer to get a truer thermal profile of the system almost instantaneously, without the large time lags associated with heat transfer through a thermal resistance such as a heatsink or even surrounding air.

TDM ICs such as the Analog Devices ADM1023 and ADM1032 are 1 degree Celsius accurate temperature measurement devices. Figure 2 shows how these digital sensors connect via a two-wire bus, simplifying the interface to a supervisory microcontroller or DSP.

The temperature reported back by the IC is directly related to the V_{BE} of the remote transistor (either a discrete device or embedded on-die transistor). The technique works by pushing two accurate low-level currents

▲ Figure 2. Using an ADM1023 or ADM1032 thermal diode monitor IC to achieve 1° C accurate temperature measurement.

▲ Figure 3. Monitoring multiple temperature zones in the basestation.

through the temp-sensing element and calculating the ΔV_{BE} (change in V_{BE}) of the transistor. This makes the technique immune to characteristic variations from transistor to transistor (due to manufacturing process variation). If only one current was used, each system would have to be individually calibrated to account for transistor parameter spreads. The temperature measured is given by

$$DVbe = \frac{kT}{q} \, {}^* \ln(N)$$

where k = Boltzman's constant, T = temperature in Kelvins, q = electron charge and N = ratio of the two currents.

Note that the 8-pin ADM1032 and 16-pin ADM1023 devices perform this calculation on-chip, measuring and expressing the temperature measurement in 8-bit 2's complement format. With 2's complement, bit 7 is the sign bit, allowing both positive and negative temperatures in the range of –127° to +127° C to be measured. This 8-bit value needs to be converted from hex to decimal when read from the device via the serial two-wire bus. All devices that can measure a remote temperature also have an additional temperature sensor on-chip, allowing system ambient temperature to be measured.

Revisiting the original system-level diagram of the basestation, Figure 3 proposes how the hottest components/modules in the system may be monitored using multiple ADM1023 or ADM1032 devices. In the case of the ADM1023, up to nine devices may be placed on to a single two-wire bus by rewiring the device addresses via dedicated address pins. Each device can be interrogated individually by the system SMBus master, allowing zone temperatures to be reported back. On-chip temperature limits can be programmed in for each device. If a temperature exceeds the pre-programmed limits, an interrupt is generated, alerting management software.

Cooling the basestation

Having determined how to monitor critical temperature zones in the basestation, the designer now needs to consider how to cool it. To a large extent, this will depend on the physical shape and size of the basestation. In turn, the scale of the basestation will be dependent on the amount of traffic it is expected to handle and whether it is designed for indoor or outdoor use. Indoor units for use in office buildings tend to be small, typically the size of an ATX type personal computer. Tight form-factors coupled with high-performance, highly integrated ICs limit the amount of passive air-cooling (through air inlets) or even forced cooling using fans. This makes the thermal design of the system critical if the basestation is to be adequately cooled. Larger basestations intended as central communication hubs are generally modular, giving the end customer the flexibility to upgrade to additional channels/bandwidth. However, this can mean that plugging in an extra module could change the overall thermal characteristics of the system. For example, adding a module to a rack could severely restrict or completely block airflow from a rear-mounted fan. Some components would then be running at elevated temperatures reducing system reliability.
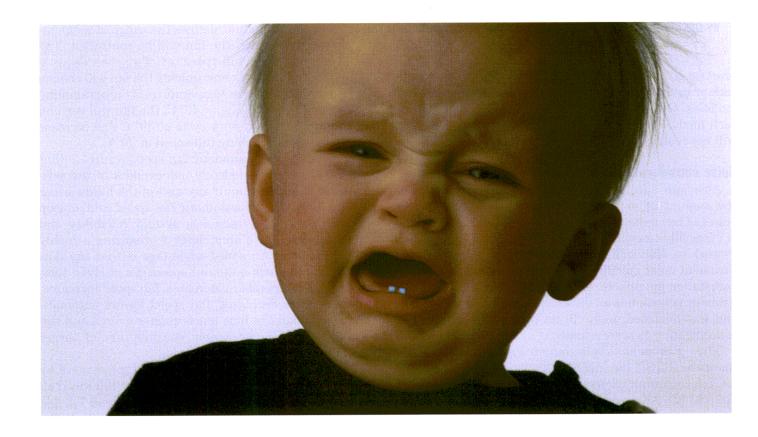
When designing fans into a basestation, a designer may use any of these three approaches:

(a) Provide all fans in the system rack, regardless of the number of modules being fitted to the rack for that customer, i.e., design and provide for worst case cooling. For example, design a large basestation with 32 fans mounted at the rear of the cabinet.

(b) Provide the required number of fans for the customer configuration. For example, if the customer orders three modules, each requiring two fans for adequate cooling then fit the rear of the system with six fans. If they add more modules later, they need to add more fans.

(c) Design the modules so that the fans are a part of the module instead of being fixed to the rear of the cabinet. When the customer purchases additional modules, they are also receiving additional fan cooling.

Option (a) has the advantage because the basestation will accommodate and cool future modules that may be added to the system. However, the system runs 32 fans when only two or four may be needed, which makes the system extremely noisy and wasteful of power. Option (b) makes more sense, since the designer fits the system with the required number of fans for the customer's configuration. On the other hand, this might not be ideal in

Operating Environment	Maximum Noise Level
Telecommunications Equipment (unattended)	75 dB
Telecommunications Equipment (attended)	72 dB
Business Area (> 4 m from desk work locations)	68 dB
Business Area (< 4 m from desk work locations)	63 dB
Office (floor-standing equipment)	55 dB
Office (desktop equipment)	50 dB
Power Room	83 dB

▲ **Table 1. Acoustic standards for telecommunications equipment set by the European Telecommunications Standards Institute (ETSI).**

practice if the designer wants to manufacture a single rack or backplane and just plug in the desired number of modules. Option (c) seems to be the best choice, since each module will be responsible for its own cooling and will not restrict the airflow of other modules.

Noise considerations

Although adequate cooling is the primary concern, the amount of noise the basestation will make when powered has to be taken into consideration as well. This is especially important if the system is an indoor unit located in the vicinity of office desks and workers. Stringent noise guidelines have been laid out, and every basestation manufacturer should attempt to meet them. Acoustic pollution is an unwanted distraction and is less and less tolerated, with effects ranging from lapses of concentration to severe stress.

The European Telecommunications Standards Institute (ETSI) has defined acoustic noise guidelines for telecommunications equipment in document ETS 300 753 [2]. All acoustic noise measurements are taken in accordance with ISO7779. Table 1 lists the acoustic noise requirements based on the expected operating environment of the telecommunications equipment.

The easiest and most effective way to reduce the amount of noise from the basestation is to turn on the fans only when cooling is required. Since temperature is measured, this becomes easy to do.
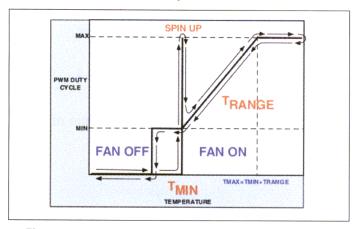
Automatic fan speed control

The basestation could be designed so that its fans switch on automatically full-speed at a certain temperature, but this would make the system very loud. Several Analog Devices system monitor products integrate temperature measurement with an automatic fan speed control function. The designer can program the starting temperature, T_{MIN}, at which the fan should switch on. The designer can also program a T_{RANGE} value; this defines the range of temperature over which the fan will be controlled. The fan will run full-speed at $T_{MAX} = T_{MIN} + T_{RANGE}$. T_{RANGE} defines how quickly the fan will change in speed with changes in temperature. By programming $T_{MIN} = 30°$ C and $T_{RANGE} = 40°$ C, the fan will turn on and run at 33 percent duty cycle at 30° C and increase linearly in speed, reaching full-speed at 70° C.
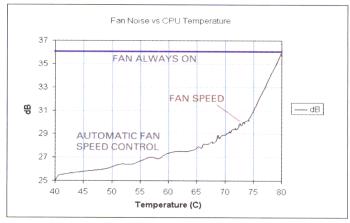
The advantage of automatic fan speed control is that the control loop is completely independent of the software after configuration. If any part of the hardware or software locks up, the automatic fan speed control loop will still work. This increases system reliability and brings the designer a step closer to realizing a highly available system. An added advantage is that the fans are running at their optimum speeds for a given temperature. As temperature increases, fan speed increases. As temperature decreases, fan speed lowers automatically. This makes the fans much quieter overall and significantly reduces the power consumption of larger basestations running multiple fans.

Figure 5 shows how the noise of a fan is enhanced by the automatic mode versus when it runs at full speed all the time. In this case, T_{MIN} was set to 40° C and T_{RANGE} to 40° C, so the fan would reach full-speed at 80° C. The noise was up to 10 dB lower than if the fan had been running full-speed continuously.

Scaleable systems

The ADM1029 is an example of a temperature moni-

▲ **Figure 4. Automatic fan speed control function.**

▲ **Figure 5. Automatic fan speed control reduces the base-station's acoustic noise.**

Figure 6. Diagram of the ADM1029 standalone in a system without a two-wire serial bus.

tor and automatic fan speed controller for use in scaleable basestation designs. This device can monitor two remote temperatures and control two fans independently. Up to eight of these devices can be hung on to the same two-wire serial bus, allowing complete control of up to 16 fans. Intelligent fault signals allow other fans to spin automatically should another fan in the system fail, or be unplugged. This device also allows remarkable flexibility because the automatic fan speed control function even works in systems where there is no two-wire serial bus available to program the device. The device can instead be programmed using two resistors, as shown in Figure 6.

The ADM1029 is ideal for basestation designs that are intended to be scaleable. One ADM1029 could be placed on each module in the rack, controlling two fans on each board. Each fan can be controlled independently from a different thermal source, or the hottest temperature measured in the system can control both fans. It is ideal for use in systems that require extremely high fault tolerance. The device has a cascadable fault pin, CFAULT, that can signal to other ADM1029s on other modules through the system backplane. If any fan fails or is unplugged, fans on other modules can be run at higher speeds automatically to compensate for the loss in system airflow.
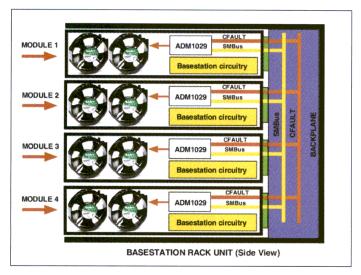
The device is intelligent enough to know when fans are hot-plugged or unplugged from the system. The device also features a unique fan freewheeling test to verify the operation of both fans connected to it. If a fan is in close proximity to another fan (which is broken), the second fan spins due to the windmill effect, i.e., the airflow from the first fan through the second fan causes it to spin. The ADM1029 will spin up each fan independently and measure their speeds to detect failed fans.

Figure 7 shows how multiple ADM1029s can communicate along a common bus or backplane, allowing an extremely fault-tolerant system.

Keeping track of supplies

Even though larger outdoor basestations may be air-cooled, the overall system reliability and absolute need for 24/7 operation, along with predictive failure, ensure the need for systems management. Equally as important as temperature measurement is the measurement of system voltages and currents supplied by the power supply unit. Any out-of-limit voltage needs to be detected and acted upon as this can indicate imminent power supply failure. If a failure can be predicted, pre-emptive action such as switching over to a redundant power supply or generating a warning message to network management software can be taken. This will reduce the likelihood of system downtime and increase system reliability.

A number of devices that measure temperature also have the capability to directly measure system power supply voltages, such as +2.5 V, +3.3 V, +5 V, +12 V and –12 V. Alternatively, voltage dividers may be added external to these devices to allow other common voltages to be monitored. One such example is the ADM1025 Temperature and Voltage Monitor, shown in Figure 8.

Putting it all together

Since a high availability system such as a 3G basestation would need to monitor all of these parameters and control fans, a highly integrated device must encompass all of the outlined functions. The ADM1026 ASIC can measure up to 15 voltages and eight fan speeds, supports automatic fan speed control and includes 8 kilobytes of on-chip EEPROM for holding field replacement unit (FRU) information. It is housed in a 48-pin LQFP package, which increases functionality in limited board

Figure 7. Connecting multiple ADM1029s to a common bus or backplane for a highly fault-tolerant basestation.

▲ **Figure 8. Using the ADM1025 to monitor power supply voltages in the system.**

▲ **Figure 9. An ADM1026 manages temperature, power supply voltages and control fans in the 3G basestation.**

be latched, even if the ADM1026 device or entire basestation is powered off. The event will be latched in memory and reported to the system software the next time that the ADM1026 is powered up. By appropriately setting high and low limit values for each measurement, any out-of-limit parameter will be detected and reported back to the microcontroller or CPU.

Figure 9 shows how the ADM1026 forms the basis of a complete 3G-basestation systems management solution. By communicating over a network with the device, remote management software can oversee and diagnose the 3G basestation remotely.

Conclusion

This article described how any of the Analog Devices Temperature and Systems Monitoring product range can become the core systems management supervisor and controller in a basestation design. A wide range of products exist, such as ADM1023, ADM1025, ADM1026, ADM1029 and ADM1032, to cater to the various systems management needs. Multiple temperature measurement capability allows local system thermal profiling and supervision. Voltage measurement detects power supply brownouts and can predict pending power supply failure. Integrated thermal monitoring and fan control ensures fail-safe standalone thermal management without any software overhead. Critical over-temperatures are detected so that systems can shut down as a safety mechanism. Multiple devices may be mixed on a common bus to realize a systems management supervisor that will monitor all critical parameters of the 3G basestation. ∎

References

1. The survey "User Ratings of Midrange Systems" is available online at: http://www.highavailabilitycenter.com/overview.html

2. ETSI document 300-753 is available for download from the European Telecommunication Standards Institute at: http://www.etsi.org/

Author information
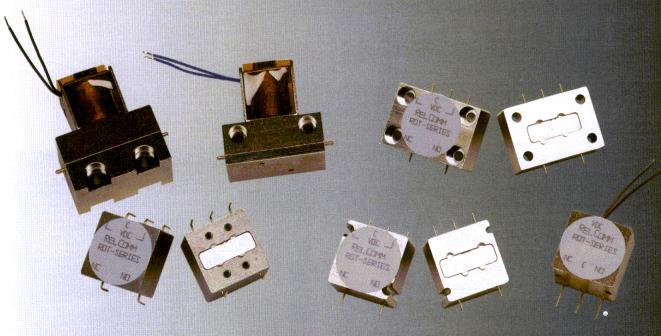
David Hanrahan is an applications engineer for the Analog Devices Temperature & Systems Monitoring Group (TSM) and is based in San Jose, CA. He has worked at Analog Devices since 1998, after completing a BTECH in electronic engineering at Waterford Institute of Technology, Waterford, Ireland. He has also published an article titled "Fan Speed Control Techniques in PCs" in *Analog Dialogue* 34-4 (2000). He may be reached by E-mail: david.hanrahan@analog.com; Tel: 408-382-3809; or Fax: 408-382-2708.

Further information on the products referenced in this article is available on the Analog Devices Temperature & Systems Monitoring Web site at: http://www.analog.com/industry/pc_pavilion/pt_monitoring/ d_center/

space. Unused fan speed channels can be reconfigured as GPIO pins. This offers increased flexibility to the hardware designer.

The ADM1026 sports extra features such as a 1.8 V or 2.5 V voltage reference to replace existing LDO circuitry and a Chassis Intrusion (CI) input to detect unauthorized tampering with the equipment. Connecting a 3-volt CMOS battery to the V_{BAT} pin allows CI events to

Product Focus — Cables, Connectors and Accessories
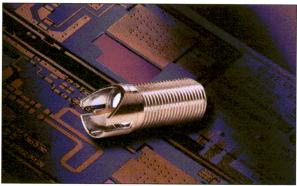
Connectors, cables and accessories are key products in the microwave and RF industry and are constantly being refined and upgraded to meet the specific needs of new applications. Here are some of the recent new products announced for this market.

Surface mount F-connector

Trompeter has introduced a new edge-mount circuit board F-connector, the CBJE130. This new connector features a center pin in-line with the plane of the board for signal integrity. The side launch design approach also allows for a

lower profile than standard right angle jacks, reducing board space requirements. Designed for broadcast and cable box products, the CBJE130 is part of the high frequency PCB coax connector series featured in Trompeter's newly released *PCB Design Guide*. Product pricing in million-piece quantities is $2.14 each.

Trompeter
Circle #188

RF connectors

HUBER+SUHNER has introduced a new generation of QUICK-FIT RF connectors

designed for quick and reliable in-field assembly in the radio base station environment. These connectors are available in N and 7/16 interfaces designed for several sizes of corrugated copper cables, including 1/2, 3/4, 7/8, 1 1/2 and 1 5/8 inch. All QUICK-FIT connectors are rated IP 68 using a three-stage sealing concept that waterproofs the jacket, outer conductor and connector interface.

HUBER+SUHNER, Inc.
Circle #189

SMA connector series

Compel Electronics has launched its SMA connector series. Operating from DC to 18 GHz, the new line offers typical insertion loss of <0.06 dB and VSWR of <1.15:1 with 50 ohms impedance. RF leakage typically measures <90 dB. Brass or stainless steel housings are available with gold, passivate or ternary alloy plating options. To facilitate numerous applications, designs are available to accommodate flexible,

TRU is on the move to heighten the personalized service, custom engineering and variety of choice you've come to expect from us since 1951. We've increased our design and manufacturing capabilities, recruited top RF engineers from throughout the industry, and streamlined our order processing systems. All this to reinforce our commitment to providing the very best in RF connectors and cable assemblies.

When your connections count— count on TRU.

This is TRU

It pays to be well connected

Circle 34

conformable and semi-rigid cable, PCB mount and panel or bulkhead mounting. All styles are available in straight, angled and swept right angle configurations.
Compel Electronics, Inc.
Circle #190

Bias Tee

Microlab/FXR has increased the current capability of its Bias Tee from 2A to 4A to meet the latest requirements of remote bi-directional and tower top amplifiers. Model HW-11N consists of an RF coaxial line that blocks DC and video, with an auxiliary shunt that has a high impedance to RF and a low impedance to video or DC power. The Bias Tee features high isolation and a 100-watt power capability over the cellular/GSM, PCS/DCS and UMTS frequency bands at 800 to 2200 MHz. A special feature of this model is the wideband isolation of the RF path from spurious DC power line interference. Model HW-11N is specified to reject all spurious signals from 500 to 2500 MHz by at least 50 dB.
Microlab/FXR
Circle #191
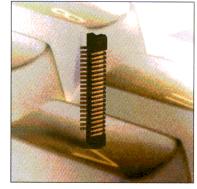
Pressure connector

Teledyne Interconnect Devices, a unit of Teledyne Electronic Technologies, now offers custom miniature high density pressure connectors in a wide assortment of configurations and materials. These low-profile, small mass connectors consist of one piece and deliver a solid gas-tight in-ter-face for dependable performance. Teledyne has reduced the turn capacity by expanding their production. This has reduced the turnaround time from prototype development to delivery. The connectors are currently available in both SMT and solderless versions; contact pitch can be specified down to 1.0 mm. Cost in volume is as low as $0.01 per contact.
Teledyne Electronic Technologies
Circle #192

Fiber optic buffer and coating stripper

Schleuniger's FiberStrip 7030 machine was specifically designed for stripping buffers and/or coatings from glass fibers with the highest possible quality or repeata-

bility. The Fiber-Strip 7030 is light and portable (1.5 lbs.) and therefore suitable for field use. Features include a precision die blade centering system, adjustable temperature heating and dwell time system and rate of controlled stripping system. Special grippers are available for use with jacketed cables; an adapter is available to accept fusion splicer fiber holders.
Schleuniger, Inc.
Circle #193

Site kits

Andrew continues the expansion of the global production and distribution of its 3G OnePack^{SM} site kits by establishing site kitting at its distribution center in Madrid, Spain. One-Pack site kits are custom-configured and contain all the components necessary for a 3G RF path subsystem in a single package. Customers can specify their own combination of Andrew RF path products. This 3G kitting service will allow 3G licensees to shorten their planning and building schedules without compromising system performance.
Andrew Corporation
Circle #194
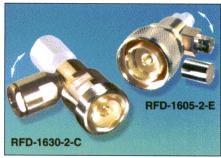
Male and female connectors

RF Connectors has announced the release of the RFD-1605-2 and RFD-1630-2 series of 7-16 DIN male and female connectors. These silver-plated, machined brass connectors with Teflon® insulation feature the versatile combination head configuration. Because the ferrule
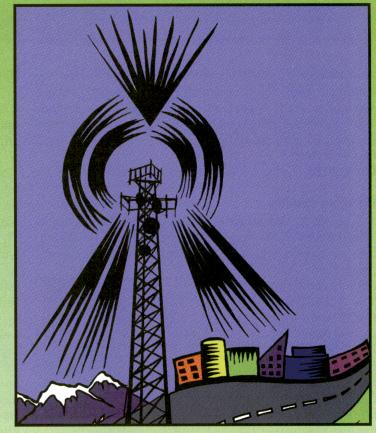
stud back-nut or cable clamp assembly screws into the connector body, the user can choose whether to create a straight or right angle connector. These ser-ies include 7-16 DIN male and female crimp and clamp connectors for most 50-ohm coaxial cables.

RF Connectors
Circle #195

Crimping systems

Autosplice has announced the availability of a new "Guillotine Cutoff" option that can be incorporated into new or previously installed crimping systems to im-prove productivity and throughput. The Guillotine Cutoff consists of a precision cut-ting blade, direct-ly integrated into the crimping head, which trims off the excess wire during the same motion as the crimping action. This new option eliminates the need for the operator to perform a secondary hand-trimming operation after crimping.

Autosplice, Inc.
Circle #196

RF coaxial connectors

Tru-Connector has introduced a series of RF coaxial connectors designed for high power military applications and high-temperature environments, such as aircraft engines. The HN-, N-, SC-, SMA- and TNC Series con-nectors can now be manufactured with Fluoroloy® H-dielectrics, which allows them to operate at up to 5,000 watts and temperatures of up to 200 degrees Celsius, depend-ing upon connec-tor type. Configurations include straight, right angle and bulkhead connectors in both male and female designs for use with semi-rigid and flexible cables.

Tru-Connector Corporation
Circle #197

Circular connectors

Amphenol® Industrial Operations has introduced a new series of connectors that provide a path for any stray voltage to be shunted to safe ground, avoiding harm to the opera-tor and voltage-sensitive equip-ment. The new Pre-Earth/First Mate Last Break (FMLB) connec-tors are ideal for applications where a protective circuit from the shell to safe ground is a safety requirement, for example, factory automation/process control and machine tool. The connectors are intermateable with MIL-C-5015 and Amphenol 97 Series styles and meet class IP67 protection against water and dust in the mated condition. Select insert patterns are certified as CE-compliant and are tested in accordance with DIN VDE 0627. Prices for the connector series begin around $5 each in quantities of 500 pieces.

Amphenol Industrial Operations
Circle #198

Digital Frequency Converters Translate Baseband to IF in 3G Base Stations

Intersil Corporation has expanded its CommLink™ family of components for software defined radio (SDR) circuits with new digital up- and down-converter integrated circuits. These devices are intended specifically for 3G cellular infrastructure, including support for smart antenna technology.

The ISL5416 is a quad-programmable digital downconverter that receives incoming wideband signals from high-speed analog-to-digital converters. The device tunes, filters and decimates the signal from an intermediate frequency band to baseband. To meet the requirements of 3G cellular systems, the ISL5416 has numerous postprocessing functions, such as automatic gain control, resampling FIR and frequency discrimination that further condition the signal before transmitting the data to the baseband processor.

The ISL5217 is a quad-programmable upconverter (PUC) that operates in the transmit section of cellular base stations. The device converts digital baseband data into modulated or frequency translated digital samples. Multiple quad-PUC can be cascaded digitally to enable up to 16 channels. The output matrix of the ISL5217 is designed to meet the flexibility requirements of smart antennas. Later this year, Intersil plans to introduce the ISL5216 downconverter, a companion part to the ISL5217 that supports the receive sections of wideband digital base stations.

These devices are part of the CommLink family of components for wideband digital radio sys-
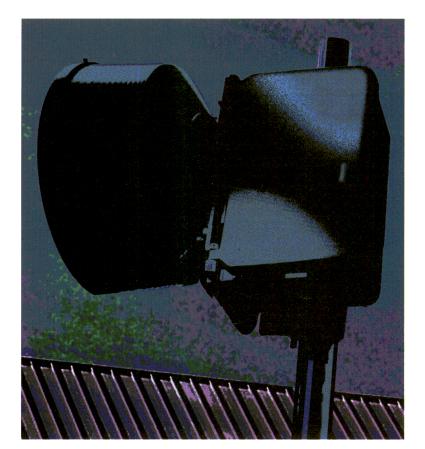
▲ Intersil expands its CommLink digital radio product line with new digital up- and down-converters.

tems. They include SDR systems that can be programmed to support legacy communication formats as well as future digital transmission protocols. The product family includes A/D and D/A converters, up- and down-converters, modulators and demodulators, direct digital synthesizers, numerically controlled oscillators and several types of filters. ■

For more information, contact:

**Intersil Corporation
2401 Palm Bay Road NE
Palm Bay, FL 32905
Tel: 1-888-468-3775, ext. 8008
Internet: www.intersil.com/design/commlink**

or circle Reader Service #200

Tiny Isolators Enable Smaller Products for Next-Generation Wireless

Murata Electronics North America has introduced a new line of ultra-compact isolators for next-generation wireless products. The CE040 series of isolators meets product designers' demands for smaller and lighter components used for wireless handsets using new standards such as WCDMA or cdma2000.

Murata has engineered numerous improvements into the new isolators, including a new structure for the inductance section, the use of original magnetic circuitry and low-loss circuit technologies. These techniques have resulted in reduced size of the isolators while maintaining performance. The new design is supported by an entirely automated manufacturing process, which allows the isolator to be provided at a reduced cost.

The CE040 isolator measures 4×4×2 mm

▲ The new CE040 series isolators from Murata Electronics North America meets designers' demands for thinner, smaller and lighter wireless components.

Frequency range	1920-1980 MHz	
Operating temp.	−35 to +85°C	+20 to +30°C
Insertion loss	A>B>0.55 dB	A>B>0.45 dB
Isolation	A>F>14 dB min.	
VSWR (forward)	A>1.6 max.	A>1.4 max.
VSWR (reverse)	A>1.6 max.	A>1.6 max.
Rated power	2.5 W max.	
Reflected power	0.6 W max.	
Impedance	50 ohms	
Attenuation	A>F>3840-3960 MHz: 12 dB min	
	A>B>E>F>5760-5940 MHz:	
	14 dB min.	
	20 dB min. (+25 to +85°C)	

▲ Summary of specifications for the 1920 to 1980 MHz CE040 isolator.

and weighs approximately 0.1 gram. Compared to Murata's previous CE052 isolator, the new model is less than two-thirds the volume and approximately half the weight. Also, the insertion loss of the new isolator has been reduced by 0.05 dB, with improved attenuation of second and third harmonics. ■

For more information, contact:

Murata Electronics North America
2200 Lake Park Drive
Smyrna, GA 30080-7604
Tel: 770-436-1300
Fax: 770-436-3030
Internet: www.murata.com

or circle Reader Service #201

Will those who paid too much for their spectrum analyzers please stand up.

It never pays to pay too much. Especially true in LMDS and broadband wireless measurement.

If customers won't spend more unless they get more, why should you? That's why Anritsu's new 40GHz MS2668C spectrum analyzer makes sense in this cost conscious environment.

The MS2668C comes with the high S/N ratios and superior distortion characteristics you need. Versatility for a range of applications; development,

Better value is no laughing matter.

- Narrow resolution bandwidths.
- 10Hz resolution bandwidth.
- High-speed time domain sweep.
- Trigger/gate circuit.
- AM/FM demodulation w/speaker.
- Centronics interface.
- Sweep signal generator.

manufacturing and field operations. A compact, lightweight design with Anritsu's 30 years' expertise and durability built-in. And a price that makes the MS2668C as easy on the budget as it is on your back. Simply no other analyzer does the job better for less.

This time, the joke's on them. Demand the highest performance for the lowest cost– the MS266X-series spectrum analyzers from Anritsu. Call 1-800-ANRITSU or visit www.us.anritsu.com today.

SAME PERFORMANCE • ALSO 30GHz MS2667C! • SAME GREAT VALUE

Linking the World
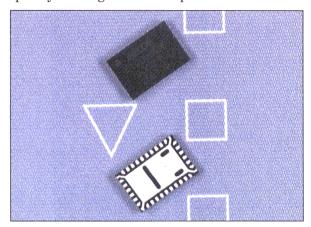
MS2668-Series Spectrum Analyzers

/Anritsu

Circle 29

FET Digital Attenuators Enable Accurate Gain and Power Control

A new family of digitally controlled attenuators has been introduced by M/A-COM, a brand of Tyco Electronics. The AT90 series includes models with 5- and 6-bit control, with 15.5 to 50 dB total attenuation and frequency coverage from DC up to 6 GHz.

▲ M/A-COM's AT90 family of digital attenuators provides many gain and power control design options.

The nine models recently introduced include integral silicon TTL/CMOS ASIC drivers for easy interfacing to the GaAs MMIC attenuator circuitry. The devices are provided in a micro leadless multichip module (FQFP-N) package that measures 6×4 mm. Features of the various models are summarized in the table below.

Pricing starts at $6.58 each in 10,000 piece quantities, and packaging can be bulk or tape-and-reel. Units mounted on test boards are available for engineering evaluation. ■

For more information, contact:

M/A-COM, Inc.
1011 Pawtucket Boulevard
Lowell, MA 01853-3295
Tel: 978-442-5000
Fax: 978-442-5350
Internet: www.macom.com
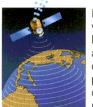
or circle Reader Service #202

Model No.	Frequency Range	Total Attenuation	Step Size	Attenuation Accuracy	VSWR (Max.)	1 dB Compression	Supply Voltage
AT90-0001	DC-6.0 GHz	31.0 dB	1.0 dB	±0.3 dB +5%	2.4:1	+28 dBm	±5 VDC
AT90-0106	DC-2.4 GHz	50.0 dB	1.0 dB	±0.5 dB +8%	2.0:1	+29 dBm	±5 VDC
AT90-0107	DC-4.0 GHz	31.5 dB	0.5 dB	±0.5 dB + 8%	2.2:1	+29 dBm	±5 VDC
AT90-0263	DC-4.0 GHz	31.0 dB	1.0 dB	±0.5 dB + 7%	2.2:1	+29 dBm	±5 VDC
AT90-0283	DC-3.5 GHz	15.5 dB	0.5 dB	±0.5 dB + 7%	1.8:1	+29 dBm	±5 VDC
AT90-1106	DC-2.4 GHz	50.0 dB	1.0 dB	±0.5 dB + 8%	2.0:1	+29 dBm	+5 VDC
AT90-1107	DC-4.0 GHz	31.5 dB	0.5 dB	±0.5 dB + 8%	2.2:1	+29 dBm	+5 VDC
AT90-1263	DC-4.0 GHz	31.0 dB	1.0 dB	±0.5 dB + 7%	2.2:1	+29 dBm	+5 VDC
AT90-1283	DC-3.5 GHz	15.5 dB	0.5 dB	±0.5 dB + 7%	1.8:1	+29 dBm	+5 VDC

▲ Summary of key specifications for nine models in the AT90 attenuator series. Some specifications vary with frequency; a review of complete product data is recommended.

Product Spotlight

How to place Product Spotlight and Classified ads in
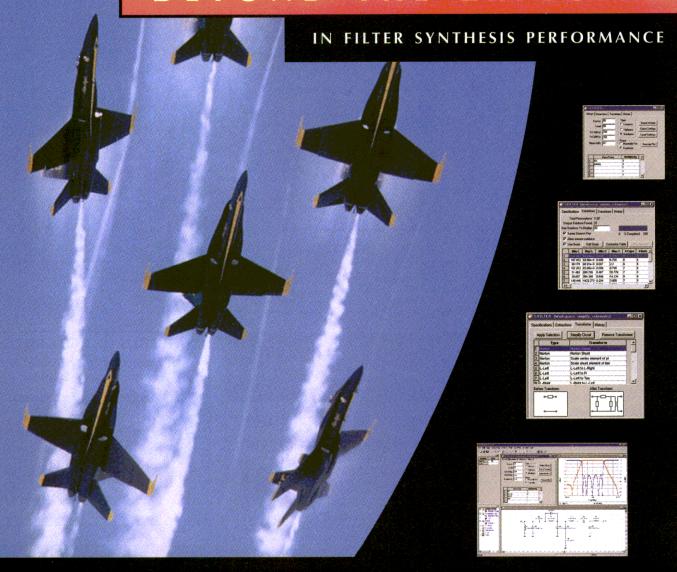
Applied
MICROWAVE & WIRELESS

Our Product Spotlight section allows you to show off your company's products or services in an economical 1/9 page color ad. Ads may be sent camera ready, or we'll make up an ad for you! All you'll need to provide is a product photo, company logo and a description of the product or service you want to advertise.

Our Classifieds section is the place to advertise career opportunities, consulting services, used test equipment and just about anything else. Special

Classifieds rates are available and are agency-commissionable if material is supplied. Or, if you prefer, our staff can make up the ad for you. Classified display ads are available in color or black and white in standard ad sizes or by the column inch.

For more information on advertising in these two sections, including rates and deadlines, please contact Aileen Kronke, Tel: 770-449-6774; Fax: 770-448-2839; E-mail: aileen@noblepub.com.

Product Spotlight

Classifieds

Advertiser Index

Tell them you saw it in
Applied Microwave & Wireless!

Market Update

Digital Television is Finally Getting Promotional Attention

The Consumer Electronics Association (CEA) has joined with the National Association of Broadcasters to implement a major digital television (DTV) promotional campaign for the fall of 2001. Consumers will finally receive the kind of information required to raise their awareness of the quality improvement and new capabilities DTV can bring to home entertainment and information.

Manufacturers of DTV products have been disappointed with the broadcast industry's efforts to delay implementation of over-the-air DTV. Without the consumer market to drive down prices, DTV would be limited to high-end audio/video buffs who may only use it with DVD movies and satellite programming. It now appears that broadcasters are ready to accept their role in the future of DTV, which includes delivery of new digital services along with standard definition television (SDTV) and high definition television (HDTV) programming.

CEA reports that 2000 sales of DTV sets and displays was 648,429 units. This information does not differentiate between commercial and consumer purchases. In 2001, sales are projected to nearly double, with larger increases in the following few years as consumers adopt DTV more quickly in response to greater availability of programming.

Technical issues

Broadcast DTV presents some of the same problems as digital cellular/PCS and even earlier digital microwave links. These include multipath (echo) effects and sudden dropouts as the receiver loses "lock" on the digital signal. Unlike analog signals, digital transmissions do not gradually fade with changing signal levels, interference or other transmission impairments.

DTV receiver manufacturers are still developing signal processing techniques to identify and cancel multipath errors. This ability will be especially important for consumers who use indoor antennas or who live in urban environments.

The development of less expensive technologies for DTV receivers and displays is key to obtaining affordable pricing. Growth in the high-resolution computer monitor market has helped speed this process by refining cathode ray tube (CRT) technology. Projection displays are presently the most affordable technique for large displays, evolving from earlier analog models. Flat-screen technologies, including LCD panels and plasma displays are available today at premium prices, but are expected to gain a significant part of the display market in the future as prices drop.

A possible transitional step with a modest cost is a mid-range display that uses a large-size CRT, but without the full 720-line progressive scan or 1080-line interlaced scan required for HDTV. This Enhanced Digital TV (EDTV) has a 480-line progressive scan resolution, which is approximately four times the resolution of present analog TV.

Regulatory and legal issues

The FCC target of 2006 for a completion of the broadcast changeover to DTV is under attack. Supporters of the deadline note that set-top boxes will be available that allow current analog TV sets to receive digital signals. With 67 percent of U.S. households hooked up to cable, many consumers will not need that new set top box to continue using an older analog TV set.

A small amount of uncertainty surrounds the "must carry" provisions of the 1992 Cable Act. Broadcasters and the CEA interpret that law as extending to new forms of broadcast transmission such as DTV. Clarification of the law may be required to assure that cable systems provide programs in the same format (for example, HDTV) as their origination.

Copy protection, an issue with the prior technologies of VCRs, audio CDs and DVDs, is also a concern with DTV. The problem essentially disappeared with the older VCR and CD technologies as prices fell to the point where there was no economic incentive to make unauthorized copies. Still, the complex issue of fitting traditional copyright protection standards to new technologies will need to be resolved, and, with any luck, without any significant delay in DTV market development.

The upcoming promotional activity will certainly raise consumer awareness, which may provide the impetus to resolve outstanding technical and legal issues. Then consumers can begin to enjoy the benefits of the dramatically higher video and audio quality of DTV. ■

> **Television broadcast networks now offer just 3.6 percent of their programming (21 hours a week) in HDTV.**
>
> *Source: "Analysis of Broadcasters' High Definition Programming Activity," Digital Tech Consulting, March 30, 2001.*

Expertise

Our Expertise — Coaxial Assembly Technology.
We have been supplying RF and microwave interconnection
solutions for the most sophisticated
airborne military electronic systems
in the harshest environments for
more than 50 years. With our
unmatched engineering and
production capabilities we can
also provide the most cost effective coaxial assemblies
for commercial applications. Get the benefit of
our expertise, call us with your application at
1-800-TMS-COAX or visit our web site at
www.timesmicrowave.com.

TIMES MICROWAVE SYSTEMS
A Smiths Industries company

ISO 9001

Circle 75